
Method development in Supercritical Fluid Chromatography (SFC) using Design of Experiments (DoE) and Design Space (DS): Application to the separation optimization of an anti-epileptic drug substance and its impurities.

Auteur : Nguyen, Amélie

Promoteur(s) : Tyteca, Eva

Faculté : Gembloux Agro-Bio Tech (GxABT)

Diplôme : Master en bioingénieur : chimie et bioindustries, à finalité spécialisée

Année académique : 2016-2017

URI/URL : <http://hdl.handle.net/2268.2/3045>

Avertissement à l'attention des usagers :

Tous les documents placés en accès ouvert sur le site le site MatheO sont protégés par le droit d'auteur. Conformément aux principes énoncés par la "Budapest Open Access Initiative"(BOAI, 2002), l'utilisateur du site peut lire, télécharger, copier, transmettre, imprimer, chercher ou faire un lien vers le texte intégral de ces documents, les disséquer pour les indexer, s'en servir de données pour un logiciel, ou s'en servir à toute autre fin légale (ou prévue par la réglementation relative au droit d'auteur). Toute utilisation du document à des fins commerciales est strictement interdite.

Par ailleurs, l'utilisateur s'engage à respecter les droits moraux de l'auteur, principalement le droit à l'intégrité de l'oeuvre et le droit de paternité et ce dans toute utilisation que l'utilisateur entreprend. Ainsi, à titre d'exemple, lorsqu'il reproduira un document par extrait ou dans son intégralité, l'utilisateur citera de manière complète les sources telles que mentionnées ci-dessus. Toute utilisation non explicitement autorisée ci-avant (telle que par exemple, la modification du document ou son résumé) nécessite l'autorisation préalable et expresse des auteurs ou de leurs ayants droit.

**METHOD DEVELOPMENT IN SUPERCRITICAL
FLUID CHROMATOGRAPHY USING DESIGN OF
EXPERIMENTS AND DESIGN SPACE:**

**APPLICATION TO THE SEPARATION
OPTIMIZATION OF AN ANTIEPILEPTIC DRUG
SUBSTANCE AND ITS IMPURITIES**

AMELIE NGUYEN

MASTER THESIS SUBMITTED TO OBTAIN THE DEGREE OF MASTER IN BIOENGINEERING
SCIENCES: CHEMISTRY AND BIOINDUSTRIES

ACADEMIC YEAR 2016-2017

PROMOTOR: Pr. E. TYTECA

SUPERVISORS: D. DIDION (UCB Pharma) and C. GALEA (Vrije Universiteit Brussel)

Acknowledgments

This study has completed many years of a great adventure...

First, I would like to express my gratitude to UCB pharma for the internship opportunity and for providing me a prestigious learning and professional environment. In this context, I would like to particularly acknowledge David who in spite of being extremely busy with his duties, took time out to hear, guide and keep me on the correct path during these five months, always with a smile. SFC has almost no more secret for me thanks to you!

My deep gratitude goes to my professor, Eva who trusted me and gave me the possibility to work on this interesting project. I would also like to thank Charlene who gave me meticulous advice, a structured scientific approach and helped me to accomplish this challenging task. Thank to both of you for the last minute corrections!

I am also grateful to have the chance of meeting so many wonderful people and professionals from whom I learned a lot and with whom I spent really good moments. Big up to the PP team: Mamy, Jo, Valérie, Vanessa and Marie. Thank you Dimitri for your precious statistical advice!

I would like to thanks all the crazy housemates with whom I shared these amazing years of University!! KDR ♥ My dear friends with who I shared parties, laughs, tears, stress, love, and many more, especially during these last challenging weeks. I would also like to thank my teammates for the relaxing moments and team work (especially during late nights when the lab lights were off).

I'm grateful to my parents and my sister for always loving and supporting me, no matter of how annoying I could be ☺ Finally, I acknowledge Guillaume who I met during my first year of University and never left since. A beautiful soul I hopefully am going to share exciting life projects with.

Thank you all, Merci, Cà m on, Dankje, Gracias, Grazie, Misaotra anoa...

Abstract

In the context of promoting green chemistry, an optimized method was developed using Supercritical Fluid Chromatography (SFC) associated to Design of Experiments (DoE) methodology and Response Surface Modeling (RSM). In this study, the performance of SFC was challenged by a real pharmaceutical case-study, which was applied to the optimal separation of an anti-epileptic drug substance and its impurities. The first step included a screening of different injection solvents, stationary phase chemistries (columns packed with sub-2 μ m particles) and mobile phase compositions. To this end, a full factorial design was carried out. The combination of CPME as diluent solvent, 1-aminoanthracene as stationary phase and a mobile phase composed of mainly CO₂ and methanol + 2% of water as modifier provided the best peak shapes with acceptable values for the tailing factor (t_f), maximized peak capacity (P_c) and peak height (h). Secondly, the method was optimized by investigating the percentage of water as additive in the mobile phase composition (%H₂O), the backpressure (BP), and the gradient time (t_G) over a predefined experimental domain in order to find the optimal separation. Therefore, all 17 drug compounds were eluted within 6.6 min gradient time when setting the backpressure at 120 bar and adding 2% of H₂O as additive in the mobile phase. DoE was used to perform the experiments. Retention times at the peak apex (RT), at the peak start (RT_{start}), at the peak end (RT_{end}) and peak width at half height ($w_{0.5}$) were modeled for 216 conditions over the experimental domain. Based on these responses, two critical quality attributes (CQAs) were computed: the minimal resolution (Rs) and the minimal separation (S) criteria. The two approaches and their respective resulting number of coelutions predictions were compared to determine the design space (DS) providing optimal separation conditions. Excel® was used to process all data and to simulate the predicted chromatograms, easing the application of this study outcome to other case studies. Once again, SFC associated to DoE and computer-assisted optimization methodology was demonstrated to be a powerful tool and a green alternative for method development in the context of impurity profiling.

Résumé

Dans un but de promouvoir la chimie dite « verte », une méthode optimisée a été développée en utilisant la chromatographie en phase supercritique (SFC) associée à la méthodologie des plans d'expériences (DoE) et à la modélisation des surfaces de réponse (RSM). Dans cette étude, la performance de SFC a été mise à l'épreuve par une véritable étude de cas pharmaceutique, appliquée à la séparation optimale de la substance active d'un médicament antiépileptique et de ses impuretés. Il s'agira d'abord de cribler différents solvants d'injection, des colonnes de différentes chimies (et faibles diamètres de particules) et plusieurs compositions de phase mobile par un plan factoriel complet. La combinaison résultante composée du CPME comme solvant de dilution, de la colonne 1-aminoanthracène (1-AA) et d'une phase mobile incluant essentiellement du CO₂ supercritique et du méthanol +2% H₂O en tant que co-solvant a permis d'obtenir les meilleures formes de pics avec des valeurs acceptables de facteur d'étalement (t_f) et des capacités de pics (P_c) et hauteurs de pics (h) maximisées. Ensuite, la méthode a été optimisée en étudiant la variation du pourcentage d'eau utilisé comme additif dans la composition de la phase mobile (%H₂O), de la contre-pression (BP) et du temps de gradient (t_G) sur un domaine expérimental prédéfini, permettant une séparation optimale. Par conséquent, les 17 composés pharmaceutiques ont tous été élués en moins de 7 min de temps de gradient lorsque la contre-pression était maintenue à 120 bar et avec une phase mobile contenant 2% H₂O. Les expériences ont été effectuées à l'aide de DoE. Les temps de rétention au sommet des pics (RT), en début de pics (RT_{start}), en fin de pics (RT_{end}), et la largeur à mi-hauteur de pic ($w_{0,5}$) ont été modélisés pour 216 conditions chromatographiques dans le domaine d'expériences. Sur base de ces réponses, deux attributs essentiels de la qualité (CQAs) ont été calculés : la résolution minimale (R_s) et le critère de séparation (S). Les deux approches et le nombre de coélutions prédit résultant, ont été comparés pour déterminer la surface de réponse optimale du design (DS). Excel® a été utilisée pour traiter toutes les données et simuler les chromatogrammes prédits, facilitant l'application de l'approche abordée dans cette étude à d'autres cas ou laboratoires. Encore une fois, la SFC associée aux DoE et à la méthodologie assistée par ordinateur a été démontré comme un outil puissant et une alternative écologique dans le développement de méthodes appliquées à l'établissement de profil d'impuretés.

List of abbreviations

1-AA	1-aminoanthracene
2-PIC	2-picolyamine
AA	Acetic Acid
ACN	Acetonitrile
ANOVA	Analysis of variance
API	Active Pharmaceutical Ingredient
BEH	Bridged Ethylene Hybrid
BSM	Binary Solvent Manager (Waters UPC ² module)
CCM	Convergence Manager (Waters UPC ² backpressure regulator module)
CM	Column manager (Waters UPC ² module)
CO₂	Carbon Dioxide
CPME	Cyclopentyl Methyl Ether
CQAs	Critical Quality Attributes
DEA	Diethylamine
DoE	Design of Experiments
EMA	European Medicine Agency
FA	Formic Acid
FAMES	Fatty Acid Methyl Esters
FDA	Food and Drug Administration
GC	Gas Chromatography
H₂O	Water
HPLC	High Pressure Liquid Chromatography
IPA	Isopropanol
ISM	Isocratic Solvent Manager (Waters UPC ² module)
LC	Liquid Chromatography
MeOH	Methanol
MS	Mass spectrometry
N₂O	Nitrous oxide
PDA	Photodiode Array detector (Waters UPC ² module)
QbD	Quality by Design

QC	Quality Control
QDa	Quadrupole Dalton mass detector (Waters UPC ² module)
RI	Refractive Index
Rs	Resolution
RSM	Response Surface Modeling design
S	Separation criterion
SFC	Supercritical Fluid Chromatography
SM	Sample Manager (Waters UPC ² module)
TEA	Triethylamine
TFA	Trifluoroacetic Acid
UCB	Union Chimique Belge
UPC²	Ultra Performance Convergence Chromatography (SFC instrumentations)
UV	Ultraviolet
Vis	Visible
WHO	World Health Organization

Table of contents

Acknowledgments.....	3
Abstract.....	4
Résumé.....	5
List of abbreviations.....	6
Table of contents.....	8
I. Introduction.....	1
II. Literature review.....	3
1. Compounds.....	3
2. Supercritical fluid chromatography.....	5
2.1. Introduction to SFC.....	5
2.1.1. Fundamental principle.....	5
2.1.2. Instrumentations.....	6
2.2. The mobile phase.....	7
2.2.1. Carbon dioxide.....	7
2.2.2. Organic modifiers.....	7
2.2.3. Additives.....	10
2.3. The stationary phase.....	11
2.3.1. Generalities.....	11
2.3.2. Selection of the column.....	11
2.4. The injection solvents.....	12
2.5. SFC versus HPLC.....	14
2.6. Applications.....	15
2.6.1. Achiral separations.....	15
2.6.2. Chiral separations.....	16
3. The detection.....	17
3.1. Photodiode array detection.....	17
3.2. Mass spectrometry.....	18
3.2.1. Ionization sources.....	18
3.2.2. Quadrupole mass analyser.....	19

4.	Design of experiments (DoE)	20
4.1.	Introduction	20
4.2.	General concept	20
4.3.	Strategy	20
5.	Design space	23
III.	Objectives	24
IV.	Materials and methods	25
1.	Instrumentations	25
2.	Chemicals	25
3.	Software	25
4.	Samples preparation	26
5.	Detection	26
5.1.	Detectors selection	26
5.2.	Compounds data	27
6.	Screening of injection solvents, stationary phases and mobile phases	27
6.1.	Full factorial screening methodology	27
6.1.1.	Objective definition	27
6.1.2.	CQAs definition	28
6.1.3.	Full factorial screening	29
6.2.	Screening chromatographic conditions	30
7.	Method optimization	31
7.1.	Objective definition	31
7.2.	Selection of the analytical chromatographic parameters	31
7.3.	Model responses and CQAs definition	32
7.3.1.	The chromatographic resolution (Rs)	32
7.3.2.	The Separation criterion (S)	33
7.4.	Chromatographic conditions of optimization	33
7.4.1.	Design creation	35
7.4.2.	Model creation	36
V.	Results and discussion	38
1.	Screening of injection solvents, stationary phases and mobile phases	38
1.1.	Full factorial design	38
1.1.1.	Injection solvent selection	38

1.1.2.	Mobile phase selection	41
1.1.3.	Column selection.....	42
1.2.	Screening of alternative stationary phases	43
1.3.	Resulting screening chromatographic conditions and compounds identification	45
2.	Method optimization	46
2.1.	Experiments and model validation.....	47
2.1.1.	Control experiments	47
2.1.2.	Modeling	48
2.2.	Design space and optimal chromatographic condition selection.....	51
2.2.1.	Resolution criterion (Rs)	51
2.2.2.	Separation criterion (S)	52
2.3.	Confirmatory experiments.....	53
2.3.1.	Responses evaluation	53
2.3.2.	Rs and S evaluation.....	54
2.4.	Optimal separation	56
VI.	Conclusion.....	59
	Bibliography.....	I

I. Introduction

According to a report published by the World Health Organization (WHO), epilepsy affects 50 million of people in the world (60 000 Belgians) ('WHO | Epilepsy', 2017). Epilepsy is defined as a neurological disorder that is caused by brain dysfunction and results in recurrent seizures. Because this type of symptom is so unpredictable, it affects the daily life of people who suffer from it, as well as their family and their friends. Even usual activities such as having a bath or driving are liable to be impacted. With this in mind, this thesis contributes to the development of an epilepsy treatment for partial-onset seizures. This inspiring project was carried out at UCB (Union Chimique Belge) Pharma, a biopharmaceutical company, focused on treatments for such severe diseases (neurological disorders, inflammatory diseases and oncology).

Nowadays, the development of a drug is one of the most complex and challenging processes that involve analytical chemistry. When synthesizing the active pharmaceutical ingredients (APIs) and drug products, they have to contain a defined quantity of API and may include impurities which must both be qualitatively and quantitatively assessed by chemical analysts. Therefore, appropriate methods have to be developed and validated for the routine quality control (QC) of drug substances and drug products under strict regulations. The standards for pharmaceutical analysis are established by organization such as the European Medicines Agency (EMA) and the Food and Drug Administration (FDA). A key difficulty in impurity analysis, results in the various physico-chemical properties (e.g. logP, solubility, pKa) of impurities, their chemical structures similarity with the active molecule and often, the trivial amounts involved.

In this context, analytical separation techniques play a crucial role. Currently, high pressure liquid chromatography (HPLC) is commonly used for QC analysis and method development for impurity profiling. Another technique, supercritical fluid chromatography (SFC), has already proven its worth but is still hardly exploited in the pharmaceutical industry. However, driven by the need to satisfy more and more standard requirements, SFC has stood out with its many advantages including fast analysis times, high efficiency, low operating costs, environmental friendliness (Berger, 2015). Indeed, using mainly carbon dioxide (CO₂) as mobile phase, this technique requires less organic

solvent which widespread use can be harmful to the environment. At the end, this separation technique can be considered as a valuable orthogonal method to the most commonly used analytical applications as liquid chromatography (LC) and gas chromatography (GC) (Nováková *et al.*, 2014).

Regarding the method development, it consists of several steps that can be sometimes tedious. It usually includes screening of important parameters in SFC, which could be the selection of the stationary phase, the modifier and the injection solvent (Dispas *et al.*, 2016). Screening studies could be followed by method optimization which can be achieved in two ways: using the traditional trial-and-error approach or design of experiments (DoE) ((Rafamantanana *et al.*, 2012). For many years, researchers used to perform their experiments in a sequential way by investigating one factor at a time, which method has ended up to be very time consuming. On the other hand, DoE is increasingly used and has managed to convince many scientists of its efficiency. This approach studies the effect of several factors on a process in order to find their optimum, and covers a much wider experimental domain for the same number of experiments.

This study investigates the possibilities of computer-assisted-method development in SFC using DoE. The approach was applied on to the analysis of an anti-epileptic drug and its impurities. Two critical quality attributes (resolution and separation factor) are employed and their efficiencies to find the optimal chromatographic conditions are compared.

II. Literature review

1. Compounds

Briviact® is a medicine for the treatment of partial-onset seizures in adult patients with epilepsy. The API of this medicine is named brivaracetam (Fig. 1). It has an exact mass of 212.29 g/mol and has good relative solubility in aqueous media with a logP value of 0.67. During drug substance synthesis or storage, impurities may arise and have to be separated, identified and quantified in compliance with quality and pharmaceutical standards. Seventeen impurities related to the process, the stability, or simply derivative compounds of the API were identified. They were previously isolated and are available as standard solutions, except for one, which is included in a complex matrix and has to be identified among unknown compounds.

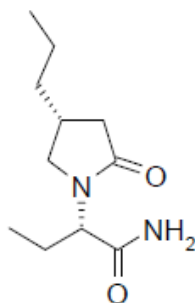


Figure 1: Chemical structure of brivaracetam

Although the molecular structures of these mentioned impurities must remain confidential, some of their properties can still be highlighted. Physical molecular properties such as logP, logD, solubility and pK_a can help to evaluate and predict the behavior of a compound for chromatographic separation, and to help establish the initial choice of some method parameters. Lipophilicity is represented by both logP, which measures the differential solubility of a compound in two immiscible solvents and logD, which measures the logP at a defined pH (Bhal, 2007). A high value of logP means that the compound is more soluble in the organic phase whereas a low value indicates a higher affinity of the analyte for the aqueous phase. This information is valuable for the type of retention strategy opted i.e. choice of column chemistry. Along with this, logD describes the change in polarity dependent on the pH, which

provides a good indication of how the retention may change according to the pH range being studied. At last, the pK_a helps to define the pH range in which a robust method can be accessed. Thus, all these properties should be considered when selecting or designing the mobile phase composition. Moreover, some of the impurities studied are thermally sensitive at temperatures above 40°C. This constitutes another parameter that should not be overlooked when developing the analytical method.

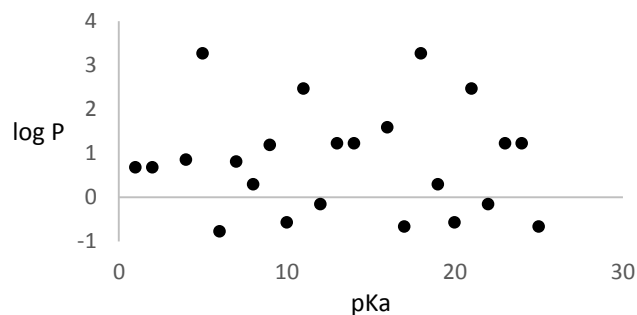


Figure 2 : Physico-chemical properties of brivaracetam and all matrix impurities. $\log P$ (lipophilicity) versus pK_a (acid dissociation constant) cover a wide range of values. pK_a includes basic and acidic functions.

The target compounds of this study cover a large range of physico-chemical properties as shown in Fig. 2. Even if most of the analytes have positive $\log P$ values, they exhibit a wide range of $\log P$ and pK_a values, making the method development even more challenging. Indeed, a large number of compounds have to be separated while a compromise has to be made for their elution. For instance, sufficient retention times for less polar species need to be achieved and at the same time, excessive retention times for hydrophilic components need to be avoided in normal phase SFC and this, with a reasonable runtime. However, the diversity encountered in this sample enhances the possibility to translate the outcome of this study to others pharmaceutical compounds.

2. Supercritical fluid chromatography

2.1. Introduction to SFC

2.1.1. Fundamental principle

SFC can be used as a preparative, an extractive or an analytical technique, but all converging to a separation technique, which working principle can be compared to high pressure liquid chromatography (HPLC) (Berger, 2015). The separation is based on the difference of the sample components affinity between the mobile phase and the stationary phase resulting in different elution time while passing through the column at high-pressure flow. However, SFC has the particularity of implementing a mobile phase composed of a supercritical fluid, with carbon dioxide (CO₂) being the most successful and common substance used, mainly due to its accessible critical point and miscibility with a large range of modifiers (Nováková *et al.*, 2014; Berger, 2015; Lesellier and West, 2015). Indeed, supercritical fluid's properties lie between those of a liquid and a gas when maintaining the temperature and pressure above its critical point. For pure CO₂, this critical point is defined by a temperature of 31°C and a pressure of 74 bar and illustrated in Fig 3 (Nováková *et al.*, 2014).

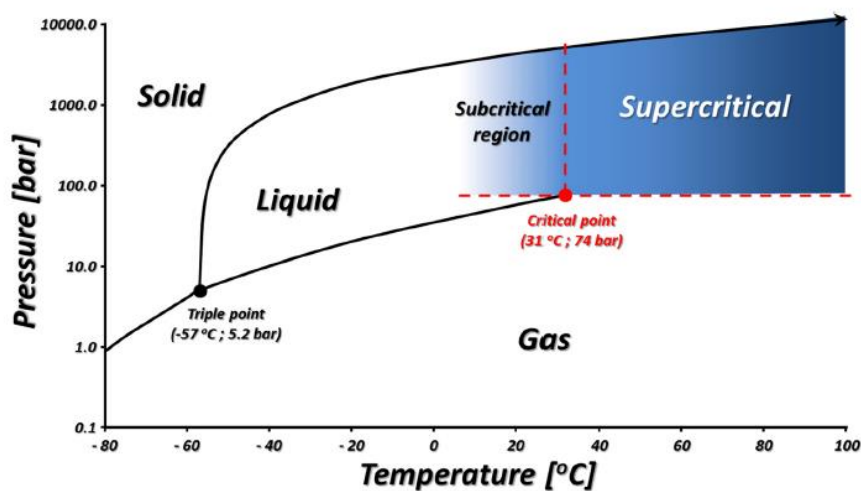


Figure 3 : Carbon dioxide diagram (Nováková *et al.*, 2014).

The supercritical fluid shows advantages of both the liquid and the gas states. As a liquid, it has a high density and solvating power, which allows lower operating temperatures and the analysis of higher molecular mass compounds. As a gas, it has a low viscosity which limits the pressure drop across the column allowing the use of longer column lengths or higher flow rate setting. It also has a fast rate of diffusion and a great optimum mobile phase velocity resulting in shorter analysis time and faster column re-equilibration. In other words, these assets contribute to high separation efficiency and fast separation capability respectively (Nováková *et al.*, 2014).

2.1.2. Instrumentations

A modern SFC system is shown in Fig. 4. This system was used for experiments of this study. Pure CO₂ is supplied from a steel cylinder at room temperature and this is chilled and compressed in a unit within the pump. As pure CO₂ has poor solvating power, small quantities of co-solvent(s), also named “modifier(s)” are often added (Lesellier and West, 2015). The mobile phase composition is then controlled by both the CO₂ and the modifier pumps. From the mixing chamber, the mobile phase is sent to the column inlet through the binary injection valves. Indeed, the auxiliary injection valve prevents liquid CO₂ entering the needle when positioning the sample onto the loop. Note that in LC, only a single injection valve is required. After elution from the column, components are then led into the Photodiode Array (PDA) detector for UV/Vis acquisition. This detector is implemented in the main flow path thanks to its non-destructive property and was chosen, inter alia, for its capability to be used at elevated pressures. A mass spectrometer (MS) was chosen as complementary detector for its high sensitivity and compound identification. The choice of detectors is further explained in the materials and methods section. This detector is destructive and placed after the splitter which has two roles: it controls the split ratio in order to avoid MS saturation and its small diameter limits the mobile phase depressurization at the column outlet.

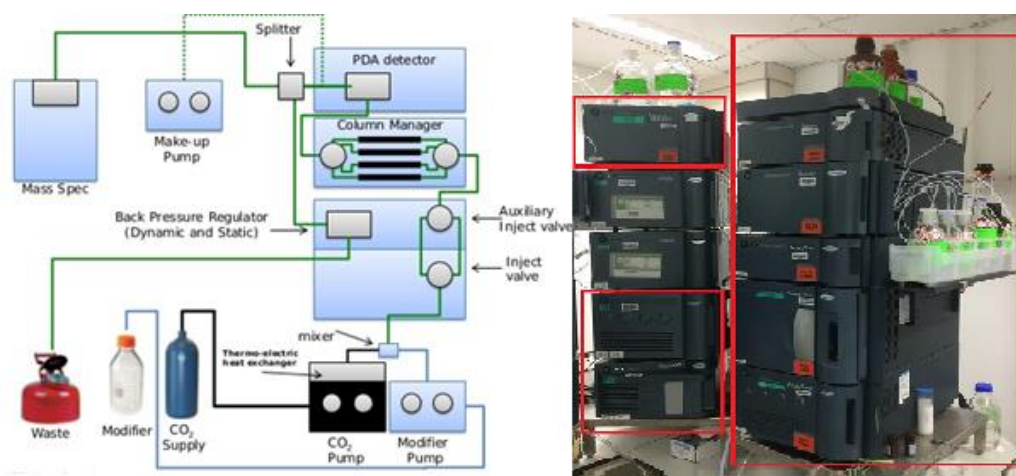


Figure 4: Acquity Ultra Performance Convergence Chromatography (UPC²) from Waters® for SFC analysis. This diagram shows the SFC instrumentation coupled to PDA and mass spectrometry detectors. The equipment used for all experiments, includes a CO₂ and modifier pumps, a mixer, a binary injection valves, a four position column manager and a back pressure regulator.

Moreover, a make-up pump regulated by an isocratic solvent manager module is required for two reasons. First, diluting the sample and then enhancing ionization before its entrance in the mass spectrometry. Especially at low modifier percentages, there is most of the time not enough ions for optimal signal detection. To this end, formic acid is added to methanol/water (80:20) solution which is used as make-up solvent. Second, it avoids the phenomenon of supercritical decompression at the column outlet. A backpressure regulator is also placed at the system outlet to limit the pressure drop of

the mobile phase throughout the entire instrumentation. The back pressure regulation is the most critical and important factor of SFC system and UV detection. It greatly affects the mobile phase density resulting in solubility and retention time changes. A modern SFC system is shown schematically in Fig. 4. This system was used for experiments of this study.

2.2. The mobile phase

2.2.1. Carbon dioxide

Numerous gases/fluids can be used as mobile phase in SFC but lots of them have many drawbacks. For instance, nitrous oxide (N₂O) has an accessible critical point (37°C and 72.3 bar) but is a strong oxidizer and mixing it with a modifier makes it explosive (Berger, 1987, 2015). Ammonia has good solvating power but is highly corrosive and leads to solid ammonium carbonate formation (Berger, 1987, 2015). Water could be an alternative since it is readily available and shows good solvating properties, but an extreme temperature (374°C) is needed to reach supercritical conditions. Compromise has to be made and it is now well established from a variety of studies that CO₂ is the best solvent for SFC (Nováková *et al.*, 2014; Berger, 2015; Lesellier and West, 2015). The reasons for this choice are multifold. CO₂ is inert towards most compounds, widely available and inexpensive, relatively safe (non-flammable and non-toxic), miscible with a large variety of organic solvents, it has low viscosity and surface tension, and weak UV absorbance at low wavelength (Ho *et al.*, 2003). As mentioned above, its critical point is accessible at a low temperature, avoiding degradation of thermolabile compounds. The polarity of CO₂ is similar to that of hexane which makes it suitable as mobile phase for the elution of non-polar compounds. On the other hand, pure CO₂ is not recommended for polar and high molecular weight molecules analysis. Furthermore, using pure CO₂ usually triggers solubility issues.

2.2.2. Organic modifiers

To tackle the issues addressed in the previous section, a small amount, generally between 2 and 40% of a more polar organic solvent is added to the mobile phase. Hence, the viscosity is enhanced leading to an increase of the internal pressure, density and solvent strength. As illustrated in Table 1, a large number of potential solvents with different elution strengths can be applied in order to fine tune the compounds' selectivity and retention times. Moreover, the use of modifier also triggers better peak shapes which results from both solubility enhancement and greater coverage of "active sites" on stationary phase such as residual silanol groups that might counteract some compounds elution (West and Lesellier, 2013; Lesellier and West, 2015).

Table 1 : Solvent selectivity for reversed-phase, normal phase, and SFC. The supercritical CO₂ is miscible with all the solvents presented for convergence chromatography, opening up a wide range of solvent selectivity choices to develop a separation ('Waters UPC²').

Solvent strength		
Solvent	Eluotropic value [E']	Polarity [P']
Supercritical CO ₂		
Pentane, Hexane, Heptane	0	0.1
Xylene	0.22	2.5
Toluene	0.22	2.4
Diethyl ether	0.29	2.8
Dichloromethane	0.30	3.1
Chloroform	0.31	4.1
Acetone	0.43	5.1
Dioxane	0.43	4.8
THF	0.48	4.0
MTBE	0.48	2.5
Ethyl acetate	0.48	4.4
DMSO	0.50	7.2
Acetonitrile	0.52	5.8
Isopropanol	0.60	3.9
Ethanol	0.68	4.3
Methanol	0.73	5.1
Water		10.2

Among the large range of solvents that could be applied as modifier, acetonitrile (ACN) and alcohols such as methanol, ethanol and isopropanol (IPA) are the most used due to their polar properties. ACN increases the retention times and contributes to poor peak capacity and peak shapes (Brunelli *et al.*, 2008). However, mixtures of an alcohol and ACN have been found advantageous for selectivity (Nováková *et al.*, 2014). Note that normal phase solvent such as chloroform and ethyl acetate, which have an environmental impact, are rarely used in SFC. Many studies have shown that methanol is the best choice for elution of polar compounds in SFC (Nováková *et al.*, 2014; Berger, 2015; Lesellier and West, 2015). The main reasons are its availability, inexpensiveness, complete miscibility with CO₂ in a wide range of temperatures and pressures (Lesellier and West, 2015), relatively low toxicity and low UV cut-off point (about 205 nm) (Berger, 2015). The gradient usually varies from 2-5% to 30-40% of modifier (Nováková *et al.*, 2014).

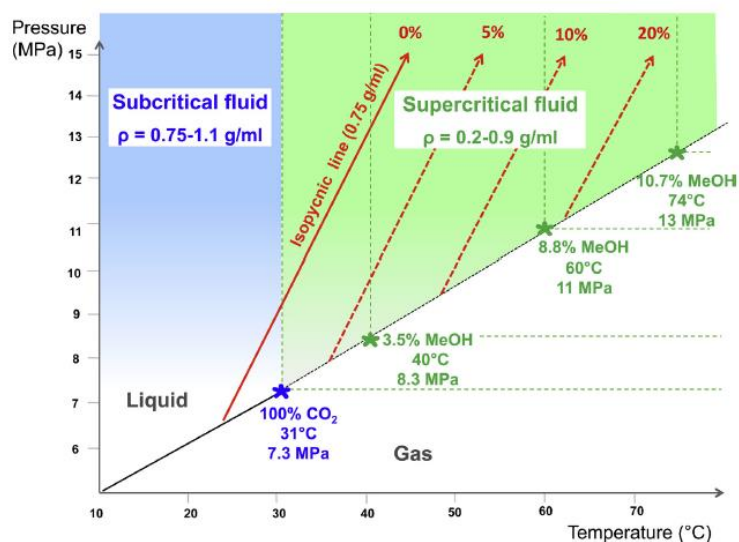


Figure 5: Phase diagram for pure carbon dioxide and different volumes of methanol. The critical point moves to higher temperatures and back-pressures as more methanol is added (Lesellier and West, 2015).

Thereupon it is important to point out that the critical point dramatically shifts depending on the nature and quantity of the modifier added. Often, the critical temperature is then not reached until the end of the gradient time and remains below the limit. Therefore, the mobile phase state is erroneously referred to as supercritical- but the correct term is in reality, subcritical. However, there is no significant impact on the separation by working in subcritical or supercritical conditions as long as the back-pressure is maintained above the critical pressure of the mobile phase composition (Lesellier and West, 2015). Hence, the temperature could remain below the critical temperature. The critical point changes of a CO₂-methanol mixture are shown in the Fig. 5. Moreover, it is usually not recommended to work in conditions close to the critical point for robust method development (Berger, 2015). In this region, little variation of temperature or pressure results in drastic changes of the density and as mentioned previously, this leads to retention and resolution variation.

Table 2: Refractive index (RI) of different substances. (‘Waters UPC²’)

<i>Refractive index</i>	
Water	1.333
Methanol	1.330
Carbon dioxide	1.000

Another reason to set the back-pressure high enough is that CO₂ and methanol have different densities and thus distinct refractive indices (RI), which are presented in Table 2. Thus, a noisy UV baseline can be observed at a low pressure due to a slight separation of mobile phase between liquid and gas when they reach the UV cell. Furthermore, the RI of CO₂ is more stable with pressures above 200 bars as shown in the Fig. 6 (Berger and Berger, 2011). This is not observed in HPLC, where water (instead of

CO₂) and methanol are used, which both have the same RI. Another consequence from this density difference is the retention changes (Lesellier and West, 2015). For all these reasons, the backpressure is typically set to a minimum of 100 bars.

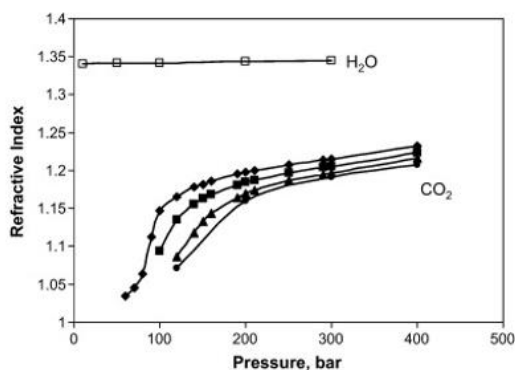


Figure 6: Refractive index vs pressure curves from top to bottom: water at 40°C, then pure carbon dioxide at 40°C, 50°C, 60°C, and 70°C (Berger and Berger, 2011).

2.2.3. Additives

Binary mixtures of CO₂ and a co-solvent such as methanol may be insufficient for the elution of very polar or basic compounds. The use of small amounts of additives dissolved in an organic modifier have a beneficial effect on the peak shapes and selectivity (Lesellier and West, 2015). The concentration range of additives usually varies from 0.1% to 2% (Berger, 2015) for organic ones and up to 10% for water (West, 2013). As a rule of thumb, basic additives such as diethylamine (DEA) and triethylamine (TEA) are often necessary to improve the peak shapes of basic compounds while acidic additives such as trifluoroacetic acid (TFA), acetic acid (AA) and formic acid (FA) are used to improve the elution of strong acids (De Klerck, Vander Heyden and Manglings, 2013). Acidic samples, though, do not always require the addition of an additive. In fact, the acidic properties of CO₂ are sometimes enough to properly elute all the sample components.

Regarding pharmaceutical compounds, they are usually known to show basic properties and aliphatic amines would be in theory, the most appropriate additives. However, mixtures of CO₂ and alcoholic modifier such as methanol may trigger the formation of methyl-carbonic acid, which pH is then approximately reduced to four or five (Zheng, Taylor and Pinkston, 2006). Therefore, an acidic additive would be the most suitable. In the context of pharmaceutical analysis, ammonium acetate (Alexander *et al.*, 2013) and ammonium hydroxide are the most recommended (Lemasson *et al.*, 2015). For both acidic and basic compounds, the use of ammonium formate are promoted (Nováková *et al.*, 2014; Desfontaine, Veuthey and Guillaume, 2016). Furthermore, attention should be paid to side reactions such as esterification when analyzing carboxylic acids, which might react with the alcohol solvent (Byrne *et al.*, 2008).

2.3. The stationary phase

2.3.1. Generalities

As mentioned in the previous section, a co-solvent is often added due to the low polarity of CO₂. When using polar stationary phases, SFC is usually associated to a normal phase technique since the mobile phase is most of the time programmed with increasing polar modifier concentration. However, when using C18 or similar columns, it cannot be referred to as reversed phase mode since the gradient is set from lower to higher polarity (Berger, 2015). Hence, SFC explores new possibilities compared to the traditional reversed phase technique.

2.3.2. Selection of the column

As the mobile phase, the nature of column is an important choice in chromatography. Retention and selectivity depend on the interactions of the sample with both the stationary phase and the mobile phase. Traditional stationary phases used in HPLC, can also be applied in SFC at the only condition of sample solubility in CO₂-based mobile phase. They include several forms of bare silica, cyano, amino, classic diol and C18 that all show a wide range of chemistries (Berger, 2015). In fact the columns intended for both SFC and HPLC, show no difference; they have the same features and are manufactured in the same way. However, some specific column chemistries such as the 2-ethylpyridine phase, introduced in 2001 by Princeton Chromatography, were specifically developed for SFC and have shown favorable outcomes (Lesellier and West, 2015). Besides this, the use of serially coupled SFC columns which have different selectivity has been demonstrated to be an effective technique for complex mixture separation (Wang, Tymiak and Zhang, 2014). Beyond any doubt, it is possible, in SFC, to go through all the polarity range with the use of the same mobile phase, which enhances the technique's diversity (Nováková *et al.*, 2014). The downside is that the large possibility of combinations makes the initial choice of column and mobile phase even more difficult since there is a global lack of knowledge about the interactions between the supercritical fluid, the analytes and stationary phases. Fig. 7 shows the large choice of matched chromatographic parameters as a function of the target-compounds polarity. In this study, almost all analytes contain conjugated ring nitrogen which makes them moderate polar compounds family.

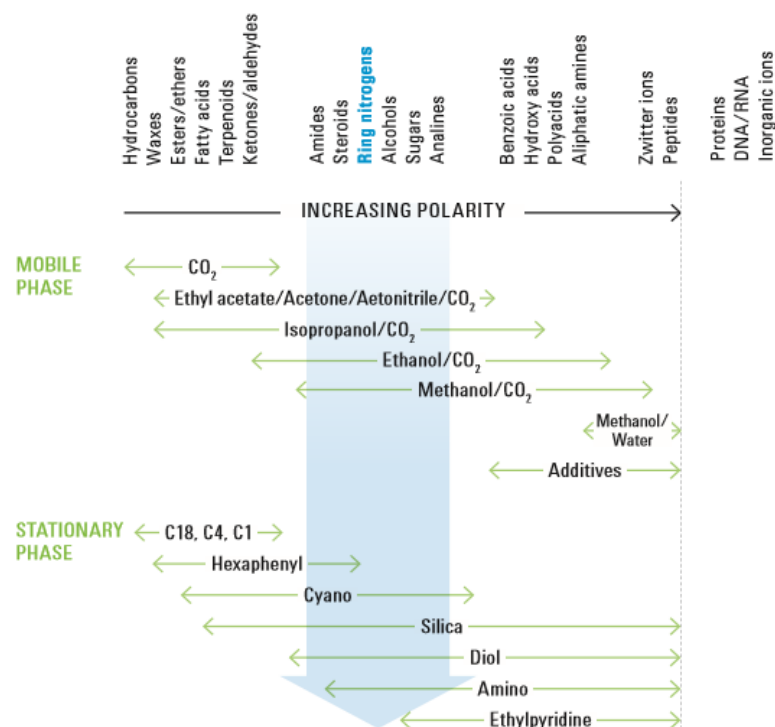


Figure 7: Suggestion of match mobile phase and stationary phase with the compounds global polarity. Compounds with increased polarity require more polar mobile and stationary phases. The vertical blue arrow targets chromatographic conditions for compounds containing ring nitrogens, which position them in the middle of the polarity scale. Source: (Berger, 2015).

In this context, the research group of Caroline West focuses their work columns ranking in SFC and has suggested classification systems allowing the comparison of hundreds of columns based on five criteria represented in a spider diagram (West *et al.*, 2015, 2016). An alternative classification method, developed for the context of drug impurity profiling, was proposed by Galea, Mangelings and Vander Heyden, (2015). However, the stationary phases used in this study are mainly characterized by big particle sizes (3 to 5 μm). Over the last few years, columns packed with 2 μm particles have shown to be interesting for high speed work. With this in mind, stationary phase ligand chemistries with sub-2 μm particles were investigated and the BEH (Bridged Ethylene Hybrid) silica and Torus 2-picolylamine (2-PIC) columns were promoted for basic drug analysis, compared to Torus 1-aminoanthracene (1-AA) and diethylamine columns (DEA) (Desfontaine, Veuthey and Guillaume, 2016).

2.4. The injection solvents

The choice of dissolution solvent plays a major role on peak shape in chromatography. Especially in reversed phase chromatography, it is widely recommended to dissolve the sample or standards to be analysed in a similar eluent compared to the mobile phase composition at the injection, in order to minimize the peak distortion. Indeed, the use of a stronger injection solvent than the mobile phase can

modify the early adsorption of the sample on the column resulting in peak broadening, fronting or tailing (Fairchild, Hill and Iraneta, 2013). In SFC, this effect is moderated by the large amount of CO₂ in the mobile phase. Even better, it has been demonstrated that a wise choice of injection solvent can improve peak shape (Desfontaine *et al.*, 2017). In fact, physical properties of dissolution solvents such as molar density, boiling point and vapor pressure have shown to contribute to sharper peaks by improving the sample dissolution in mixed CO₂-methanol phases (Abrahamsson and Sandahl, 2013). The properties of 17 injection solvents are presented in Table 3.

Table 3: Injection solvents properties. These solvents were used to dilute the samples before analysis by SFC (Abrahamsson and Sandahl, 2013).

Solvent	Boiling point (°C)	Density (g mL ⁻¹)	Vapor pressure (kPa)	Viscosity (cP)	Surface tension (dyn cm ⁻¹)	Eluent strength (ε ^o)	Dielectric constant	Dipole moment (D)	Hydrogen donor	Hydrogen acceptor
Pentane	36	0.626	57.3	0.23	15.48	0	1.84	0	0	0
Cyclopentane	49	0.751	40.0	0.44	22.42	0.04	1.97	0	0	0
Diethyl ether	35	0.713	53.6	0.224	72.8	0.29	4.33	1.3	0	0.47
Toluene	111	0.867	2.90	0.59	28.53	0.22	2.38	0.31	0	0.11
Dichloro-methane	40	1.33	47.0	0.4	26.52	0.3	8.93	1.14	0.13	0.1
Hexane	69	0.655	16.0	0.31	17.91	0	1.88	0.08	0	0
Cyclohexane	81	0.779	10.4	1	24.98	0.03	2.02	0	0	0
Acetone	56	0.791	24.6	0.32	23.7	0.43	20.7	2.7	0.08	0.43
Chloroform	61	1.483	26.2	0.57	26.67	0.31	4.81	1.15	0.2	0.1
Heptane	98	0.684	4.80	0.42	20.3	0	1.92	0	0	0
MTBE	55	0.741	25.0	0.27	19.4	0.48	2.6	1.32	0	0.3
2-Propanol	82	0.785	4.40	2.4	21.79	0.6	20.33	1.66	0.76	0.84
Tetrahydrofuran	66	0.886	20.0	0.55	26.4	0.48	7.58	1.75	0	0.55
Acetonitrile	82	0.786	9.70	0.38	19.1	0.5	37.5	3.44	0.19	0.4
Ethanol	79	0.789	5.90	1.1	22.32	0.68	24.55	1.66	0.86	0.75
Methanol	65	0.791	12.8	0.59	22.55	0.73	32.7	2.87	0.98	0.66
DMSO	189	1.100	0.056	2.24	43	0.48	46.68	4.1	0	0.76

As mentioned previously, CO₂ constitutes the main solvent in the mobile phase and has similar polarity to hexane. Following this logic, similar strong apolar solvents as heptane, cyclohexane or hexane itself would be the most appropriate diluents in SFC analysis. However, their use would not be suitable for polar or ionizable compounds' dissolution. Moreover, such volatile solvents incur the risk of evaporating during vial storage (Nováková *et al.*, 2014). It can then mislead analytes quantification since the sample becomes concentrated as the solvent evaporates. Nonetheless, these negative effects can be limited by decreasing the injection volume. Hence, it is recommended to inject a volume less than 1% of the column volume in SFC. Finally, a compromise has to be made between the sample solubility, the solvent volatility, the peak shape, the compound retention and the sample stability. The best diluent could be created by mixing miscible non-polar and polar solvent according to final gradient mobile phase. For instance, optimal peak shape of butylparaben is found by using a mixture of hexane/IPA (Fig 7A vs 7B-C).

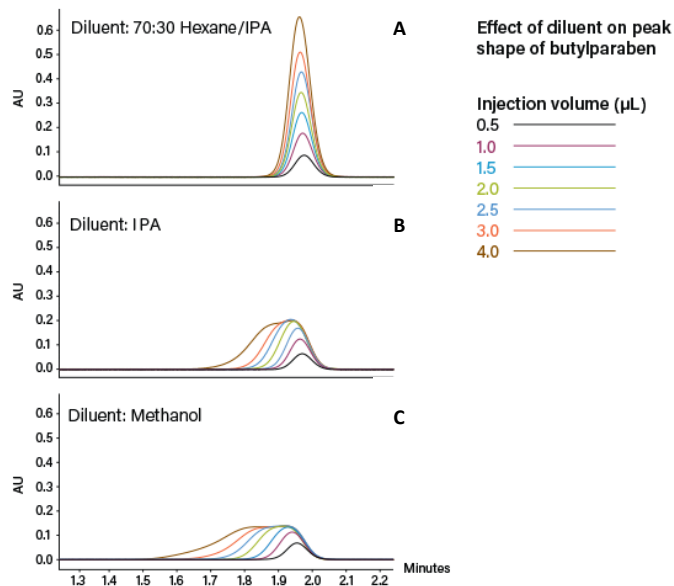


Figure 8: Butylparaben chromatogram comparison: the sample is dissolved in (A) a mixture of hexane/isopropanol, (B) pure isopropanol and (C) pure methanol (‘Waters UPC²’)

2.5. SFC versus HPLC

Until now, the most used technique for non-volatile polar or non-polar compounds analysis is HPLC. Inspired by this technique, SFC was created with the purpose of exploiting supercritical fluid properties. Indeed, such mobile phase brings a greater solubilizing power than gases in GC. In addition, the low viscosity and high diffusivity of CO₂ leads to faster analysis time and shorter equilibration times. Also, less resistance to mass transfer results in sharper peaks at higher optimum linear velocities (Cazenave-Gassiot *et al.*, 2008). This is shown by comparing Van Deemter curves presented in Fig. 8 where the optimum linear velocity for supercritical fluids is significantly greater than for eluents of HPLC. Separation can be achieved in a shorter period of time with the same efficiency or at least, without losing any resolution.

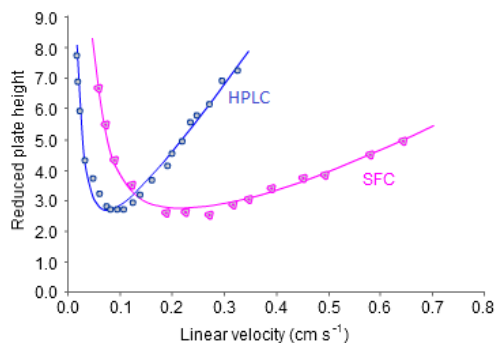


Figure 9: Plotted Van Deemter curves showing optimum linear velocity for HPLC and SFC systems. The optimal height equivalent to a theoretical plate is reached at a higher speed. Source: Brown P.R., 2005

Packed columns with reduced particle sizes have also been demonstrated to enhance optimal linear velocity and mass transfer in both techniques, but this observation was particularly drastic in supercritical conditions (Grand-Guillaume Perrenoud, Veuthey and Guillaume, 2012). However, columns packed with small particles sizes generate high pressure which has to be handled by the system. This is not always achieved since the instrumental pressure limit for the Waters® Acquity UPC² system is fixed at 414 bar, not to mention the contribution of the backpressure to maintain the supercritical state. Hence, this typical limitation could also restrict the choice of stationary phase.

Looking to another important aspect, SFC can be considered as an environmentally friendly technology. As mentioned previously, it provides rapid separation while significantly reducing the amount of organic solvent used, compared to HPLC analysis. Hence, the low quantity used is less cost-effective than usual toxic solvents but also, reduces waste disposal costs.

Despite some drawbacks, SFC is a promising technique and shows many advantages over HPLC including; shorter analysis time, less organic solvent waste, high throughput, fast calibration, greener technique but also largely compatible with a wide types of detectors which is discussed later on. Although HPLC usually offers greater peak capacities, SFC provides an alternative selectivity and is recognized as an orthogonal method to HPLC (Alexander *et al.*, 2013).

2.6. Applications

2.6.1. Achiral separations

SFC has also played an important role in the food industry. The intake of lipids, also known as fats, is crucial for human's body; they supply us with energy, are involved in the production of various hormones and many more. Their investigation is thus common but lipid analysis can be a real issue in analytical chemistry due to their complex structure. However, SFC is becoming an efficient technique for the determination of lipid composition in vegetable oils, by allowing lower temperatures analysis compared to HPLC. As an example, a method has been developed using SFC-MS technique to analyze a complex vegetable oil where 53 compounds have been identified and separated (Duval *et al.*, 2016).

Petrochemistry is another field in which SFC has been of interest. The fatty acid methyl esters (FAMES) content is limited in the jet fuel because at high concentrations, they impact the fuel thermal stability leading to gelation (Ratsameepakai *et al.*, 2015). A rapid method using UHSFC-MS was developed for FAMES quantification in aviation turbine fuel. This technique was also applied and

promoted for both separation and detection of various glycerol types in biodiesel analysis (Ashraf-Khorassani *et al.*, 2015).

SFC is also involved in food safety and international trade. In modern agriculture, the use of pesticides is an efficient way to enhance and protect crops. However, the residues from these chemical agents could end up into our food. It is therefore necessary to control pesticide residues levels in agricultural production, in order to protect consumer's health from toxic exposures. In this context, SFC hyphenated to high-resolution MS was used as a screening method to investigate multiple pesticide residues in an efficient way (Ishibashi *et al.*, 2015).

2.6.2. Chiral separations

SFC is involved in a wide range of application areas, but it is mostly known as a strong tool for chiral separations, especially in the pharmaceutical industry. Chiral molecules have the same composition and same structure, but are displayed as mirror images of one another. In the old days, many drug compounds were synthesized and sold as racemic mixtures, that means in equal concentrations of each form, supposing that one enantiomer has the active effect while the other one has no effect. It is now well established that enantiomers can have different effects, and one classical example is the thalidomide case. This medicine was administered as racemic mixture to pregnant women, while one of the enantiomer was responsible of birth defects. Since then, the FDA and other regulatory agencies have requested complete tests of each enantiomeric compound. In this context, pharmaceutical industries need to develop fast methods for drug substance development, and SFC is becoming a great option when dealing with such samples. For instance, the chiral separation of R-goitrin, which was reported to have antiviral activity, was performed 10 times faster in SFC than in NPLC as illustrated in Fig. 9 (Nie, Dai and Ma, 2016).

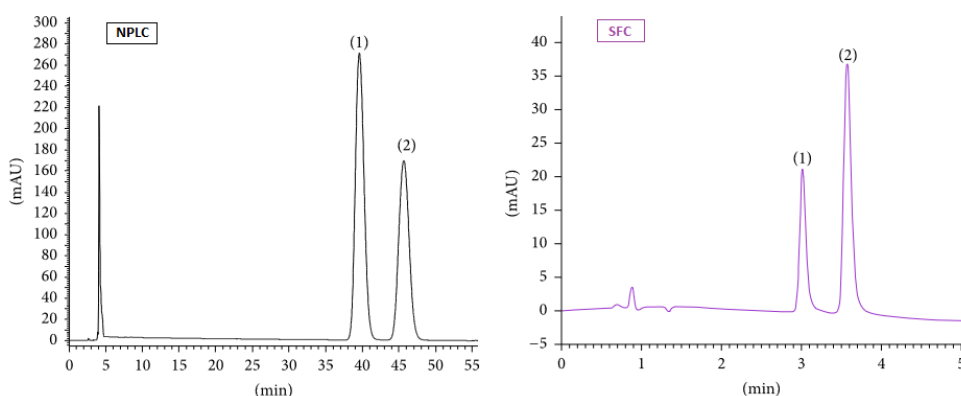


Figure 10: Chiral separation of (R,S)- goitrin with NPLC and SFC analysis. The chromatograms compared the chiral separation (1) S- goitrin and (2) R-goitrin while using NPLC and SFC methods. (Lixing Nie, 2016).

3. The detection

3.1. Photodiode array detection

The most widely used detectors are based on UV-Vis light absorbance by the analyte. UV detectors used in SFC are similar to those hyphenated to HPLC. Their success is due to their many advantages: they are cheap, robust, easy to use and have low detection limits (Crawford Scientific). They include three common categories: single or multiple wavelength and diode array detection. The last one, also named photodiode array detector (PDA), can be used in a wavelength range between 190 and 850 nm. The sample is irradiated with polychromatic light issued from a combined tungsten and deuterium lamps, through the sample, to a grating which disperses the light according to each wavelength. The array is composed of a large number of diodes, each of which measures the light intensity for a defined wavelength range depending on its position in the array (Müllertz, Perrie and Rades, 2016). The general elements composing the PDA detector are shown in the Fig 11. The absorption spectrum is finally obtained by measuring the light intensity variation through all the wavelength range. Based on the Lambert-Beer's law, the measured absorbance can be linearly related to the concentration.

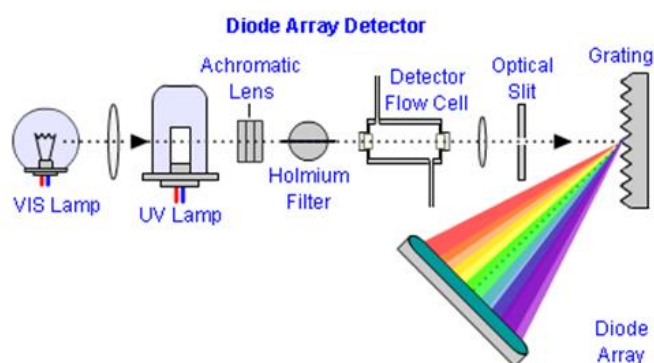


Figure 11: Components of a photodiode array detector. The diagram shows its operation (CHROMacademy).

As mentioned previously, attention has to be paid to the choice of modifier that risks UV absorbance. Also, compounds containing only C-H or C-C bonds do not show high sensitivity in UV-Vis detectors and result in a very weak signal. Hence, it is recommended to operate within a wavelength range of 200 to 210 nanometers when studying molecules that lack chromophores or/and conjugated unsaturated bonds.

3.2. Mass spectrometry

Mass spectrometry (MS) is an analytical technique that provides valuable information on molecular weight of compounds and their molecular structures. It is based on the separation of ionized sample constituents generated in an ion source. These ions are separated in the mass analyzer and then sorted by mass to charge (m/z) ratio which data is recorded by the detector. Using an internal standard, this data may help for compounds quantification as the obtained areas are proportional to their injected quantities. MS can be used alone or hyphenated to a chromatography technique (usually GC, LC or SFC) thus, becoming the chromatograph detector. This coupled method has the advantage to purify or at least, concentrate compounds of interest before their entrance in the ionization source, enhancing their detection and quantification.

3.2.1. Ionization sources

Upon leaving the SFC column and then PDA detector, it is necessary to create gas phase ions from the eluent solution for spectrometry analysis. During ions formation, one molecule may gain one electron or one ion (H^+ , Na^+ , K^+ , NH_4^+) or on the other hand, it may lose one electron or proton resulting in an ion called pseudo-molecular ions or molecular ions. While these ions are fragmented, they are named daughter ion (Menet, 2011). As a rule of thumb, molecules involving basic sites are detected in positive ion mode since they can be protonated at low pH, whereas deprotonation of an acid function at high pH leads to a negative molecular ion which can be analyzed in negative ion mode (Menet, 2011).

Several types of ionization exist and the method of choice may depend on the analyte nature and the study outcome intended. Among the oldest and popular approaches, electrospray ionization (ESI) is commonly used for polar and basic analytes, as pharmaceutical molecules.

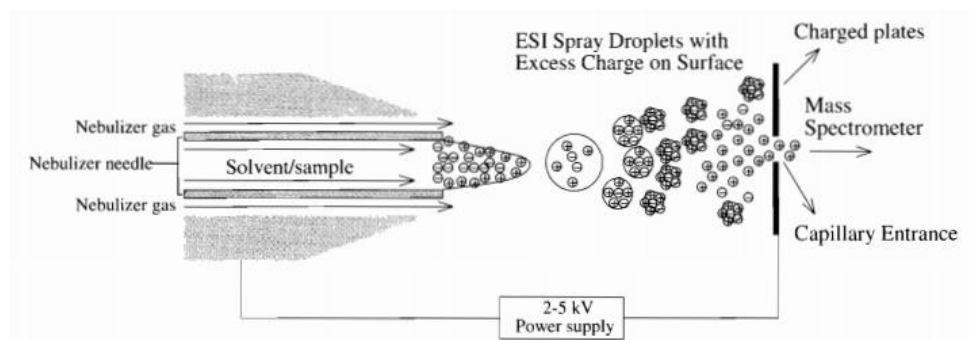


Figure 12: Electrospray instrument diagram reprinted from Silverstein. This figure shows the evaporation of solvent leading to individual ions generation.

ESI is an evaporative ionization technique where ions are generated at atmospheric pressure. The sample solution gets through a capillary tube which is surrounded by a nebulizing gas of nitrogen. The

capillary tube tip is maintained at a high voltage leading to a potential difference with the counter electrode, thus resulting in a strong electrostatic field. Therefore, highly charged droplets spray dispersion arise from the solution while exiting the capillary. Solvent evaporation is achieved by increasing temperature and/or using another stream of nitrogen drying gas, which leads to a progressive reduction of droplets size, and thereby concentrating the charged sample ions. Finally, when the electric field strength within the charged sample droplets reaches a critical point, repulsive forces go beyond those of cohesion, and droplets undergo a so-called “coulombic explosion” (Robert M. Silverstein, Francis X. Webster, 2005). At this point, surface ions of droplets have sufficient kinetic energy to be released into the vapor phase. Multiply and/or singly charged molecular ions are sampled by a skimmer cone and are then sent into the mass analyser.

3.2.2. *Quadrupole mass analyser*

The mass analyzer constitutes the heart of mass spectrometer and acts as a tunable mass filter. Its main principle rests on the separation of ions according to their mass to charge (m/z) ratio, which affects their movement through a magnetic or electrical field. Nowadays, a large majority of mass spectrometry techniques are performed with a quadrupole mass analyser. It is composed of four parallel cylindrical rods kept at equal distance. The diagonally placed pairs of rods are connected electrically, thus forming two electrodes pairs. An equal but opposite direct current (DC) voltage modified by a radio frequency voltage is applied to each pair of rods (Robert M. Silverstein, Francis X. Webster, 2005). Upon this electrical field, ions are introduced in the hollow formed by the four rods and are then, driving it along its long axis. For a set DC and modified voltage, the ions with a certain m/z ratio are capable of passing through the rods, to interact with the ion transducer and create a signal. On the other hand, all ions with different m/z values have unstable trajectory by collision with the rods or removal from the ion beam, and fail to reach the detector.

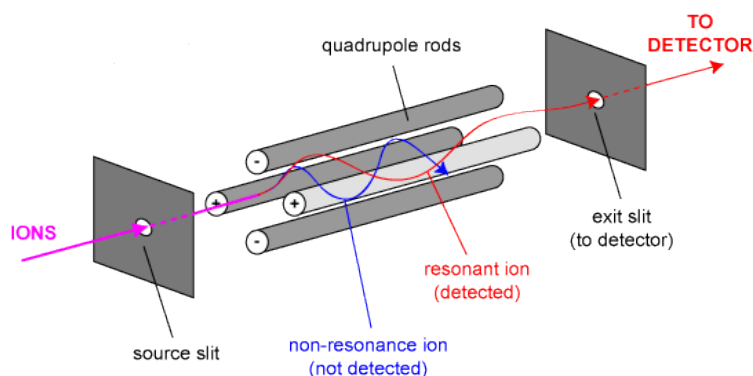


Figure 13: Operating principle of a quadrupole filter. By Dr Paul Gates, School of Chemistry, University of Bristol.

4. Design of experiments (DoE)

4.1. Introduction

DoE was born with agricultural origins in the early 1920s. It was pioneered by Sir Ronald A. Fisher, a British statistician, who also introduced the use of p-values and analysis of variances (GE Healthcare, 2014). This method shows the advantage of being less time consuming compared to the traditional trial-and-error approach that consists of varying one factor at a time. Since its beginning in agriculture, DoE has been applied across many sectors in the industry and especially, in the automotive and pharmaceutical fields. The use of statistics with randomized experiments has now become a standard method for approval of any new pharmaceutical product, procedure or medical equipment. Nowadays, DoE also contributes to the Quality by design (QbD) concept. Adopted by the FDA, QbD is applied, inter alia, for process quality in the discovery, development and manufacturing of drugs.

4.2. General concept

DoE provides a structure methodology by experiments planning to evaluate the effects, of one or several factors, on a process and its related response. This is achieved by varying several parameters simultaneously to gather a maximum of information from a minimal number of experiments (Davim, 2016). A mathematical model is then created based on the data obtained to predict responses in an experimental domain. As a rule of thumb, screening studies, optimization studies and robustness testing are the three categories of studies for which DoE is typically used. In the scope of this study, we will focus on method optimization. In this context, DoE provides the optimal design space and determines the parameters which are required to reach the critical quality attributes (CQAs) of the final procedure.

4.3. Strategy

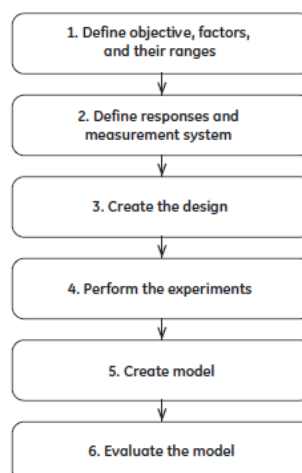


Figure 14 : Overview of DoE workflow steps. Reprinted from GE Healthcare (2014).

The strategy for DoE is drawn in the workflow shown in Fig. 14. The initial DoE step consists of defining the study objective and, identifying all relevant parameters and their levels. The second step includes the determination of one or multiple responses that map the study goal. Based on the established information, the design is created and it can be illustrated, for instance, as a cube that represents the experimental space to be investigated. The design is related to the modeling and its choice depends on the study categories (screening, optimization or robustness testing). Three related and typical experimental spaces are presented in Fig. 15.

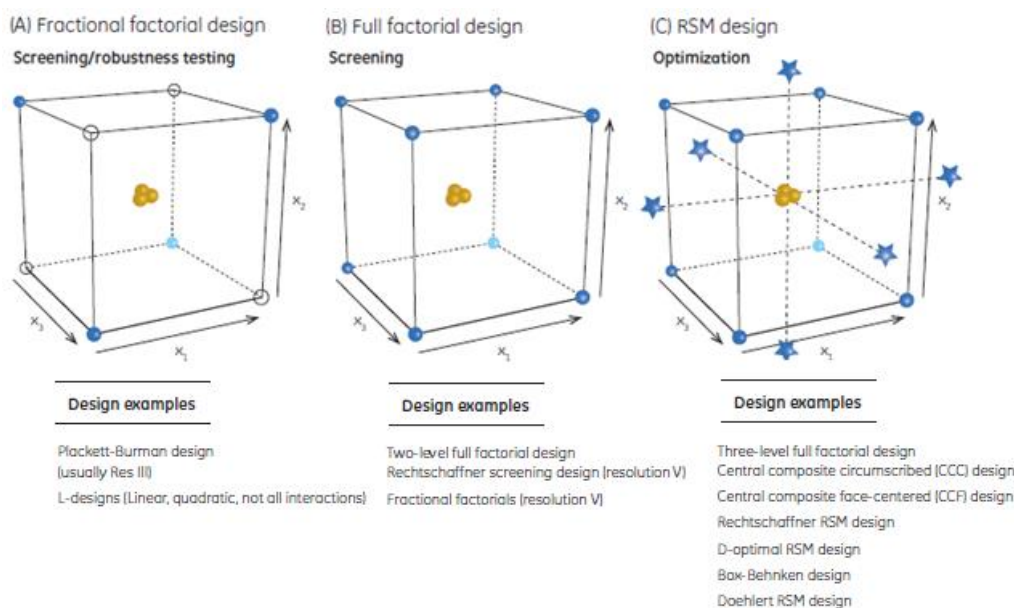


Figure 15: Comparison of typical designs in DoE and related design examples: (A) Fractional factorial design is suggested for screening or robustness testing, as the information provided only describes the main effects, which are represented by the linear terms. (B) Full factorial design takes into account all corner experiment points and is promoted for screening. This design gives information on the main factors effects and their interaction effects. (C) Response surface modeling (RSM) is used for optimization studies. This design includes the star-point experiments which investigate the curvatures of the sampling plane. This is translated by a quadratic polynomial model. Replicated center-points (in yellow) experiments are always included in the designs (GE Healthcare, 2014).

In optimization designs, more experiments are added than in screening and robustness testing. Therefore, the terms used in modeling include the main effects (first-order terms), as well as factor interactions and quadratic variables (second-order terms). Related design examples are listed in Fig.15. Among them, central composite designs are the most popular ones. They are so-called because they combine star design, center points and the two-level factorial design (Hibbert, 2012). However, the choice of design is less important than the factors and their levels, which depends on the chromatographic techniques and the compound properties.

In the next steps, experiments are performed to generate data that can later on, be transformed into figures for interpretation; this is the fundamental principle of modeling. To this end, these data are first converted into a transfer function that mathematically describes the relationships between input factors and measured responses. The transfer function commonly used is described as:

$$y = f(x) + \varepsilon$$

Where $f(x)$ describes the relationship between factors and the response (y), and ε is the error or residual term and represents the random variation that cannot be explained by the model.

For ease of understanding, a basic model containing one-factor is demonstrated. The equation becomes:

$$y = b_0 + b_1x_1 + \varepsilon$$

Where y is the measured response, b_0 represents the constant obtained at the y-axis intercept when x-axis has a value of 0, b_1 is the correlation coefficient and x_1 is the factor value.

This basic model is illustrated in Fig. 16, where the relationship between x and y is plotted. The trend line represents the optimal fit through the data. A strong correlation is obtained when all data points fall on the regression line. The difference between experimental values and predicted values is reflected by the residual error. To minimize the residuals, the least squares regression is used to calculate the correlation coefficients which value varies between -1 and +1, and where 0 indicates no correlation. A strong correlation is expressed by a high absolute value.

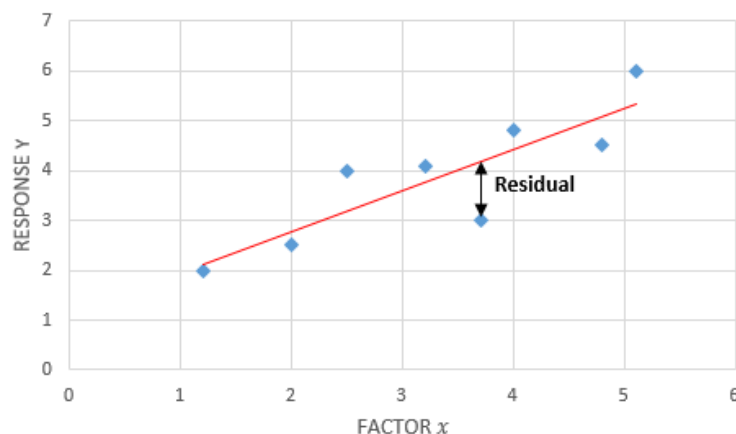


Figure 16: Linear regression analysis. The red trend line represents the model function $y = f(x) + \varepsilon$. The residual is represented on the graph and corresponds to the errors between measured data (blue dots) and theoretical predicted values (red regression line) based on the model.

In DoE, the model usually displays the relation of multiple factors on the response and grows in complexity when adding factors due to the interaction and quadratic terms. Commonly based on a polynomial function, the typical model for three-factor method optimization is described as:

$$y = b_0 + b_1x_1 + b_2x_2 + b_3x_3 + b_{12}x_1x_2 + b_{13}x_1x_3 + b_{23}x_2x_3 + b_{123}x_1x_2x_3 + b_{11}x_1^2 + b_{22}x_2^2 + b_{33}x_3^2 + \varepsilon$$

Where y is the response, b_0 is the constant term, b_n are the regression coefficients, x_n are the chosen factors and ε is the residual term. Linear terms are shown in red, interaction effects are represented in green and quadratic terms are described in blue.

Such model is applied to estimate the relevant effects by the least squares regression calculations. The obtained model can thereafter be used in predictions of responses in all experimental domains, in order to set optimal chromatographic parameters and thus, reach the initially established objectives.

However, the model relevance should always be carefully verified before making predictions and model interpretation. The model quality can be assessed by analysis of R^2 for linearity, p-values for significant coefficient and Analysis of Variance (ANOVA). The latter is a statistical test that compares the variances of values calculated by the model and the residuals. This analysis includes Fisher-Snedecor test and investigate the validity of regression and the accuracy of the model. Moreover, investigation of statistical variance between predicted and experimental responses, and normal residuals distribution gives information about the model validity (Rafamantanana *et al.*, 2012). Once the model is verified, predictions can be made and confirmatory experiments based on the model predictions are then performed.

5. Design space

Based on the RSM design, the mathematic model leads to the design space determination that can be defined as the space within the experimental domain that yields results within the set of answers reaching the initially established objective (Debrus *et al.*, 2011). Another definition could be: “*the multidimensional combination and interaction of input variables and process parameters that have been demonstrated to provide assurance quality*”(U.S. Department of Health and Human Services Food and Drug Administration, 2009), which is in this case an optimal separation of all compounds. In other words, the design space visually represents the area in the experimental domain investigated that leads to the best chromatograms.

III. Objectives

This study aims to develop an SFC-UV/MS method using design of experiments (DoE) and response surface modeling design (RSM) for the separation of the active pharmaceutical ingredient (API) brivaracetam and its 17 impurities. Such method aims to be fast, accurate, robust and selective. SFC can offer an orthogonal method compared to HPLC which is usually used in the pharmaceutical industry.

The first step of the method development included the selection of the best combination of stationary phase, organic modifier and injection solvent, which were demonstrated as crucial parameters in SFC analysis (Dispas *et al.*, 2016). This multifactorial screening was achieved with the aim of providing good peak shapes and chromatographic efficiency. Hence, the objective was to get acceptable value of tailing factor (T_f) and to maximize both peak capacity (P_c) and peak height.

The heart of this thesis resulted in the method optimization which was performed with focus on the drug and impurities separation. For this purpose, resolution (Rs) and separation criteria (S) were employed as critical quality attributes (CQAs). In this framework, the percentage of H₂O as mobile phase additive, the backpressure and the gradient time were selected as the analytical chromatographic parameters to be optimized. DoE was applied and the resulting data were used to design predictive models of half-height width, retention times at the beginning, the apex and the end of the peaks, based on which Rs and S are thereafter calculated. The models quality was statistically evaluated. Finally, the efficiency of these two approaches was compared to reach the optimal analytical chromatographic conditions.

IV. Materials and methods

1. Instrumentations

SFC analysis was performed on an Acquity Ultra Performance Convergence Chromatography (UPC²) from Waters®. The system was equipped with a binary solvent delivery pump, an auto-sampler with a fixed loop of 10µl, an Acquity column oven and a backpressure regulator (convergence manager). The system was also combined with a Photodiode array (PDA) detector, a Waters Isocratic Solvent Manager (ISM) pump and a single quadrupole mass (QDa) detector fitted with electrospray (ESI) ionization.

2. Chemicals

CO₂ (Phargalis 2, purity >99.9%) was purchased from Air liquide Carbagas AG (Domdidier, Switzerland). Methanol (MeOH) and acetonitrile (ACN) both ULC/MS grades were provided from Biosolve (France). Injections solvents were methyl tert-butyl-ether (MTBE) from Sigma Aldrich (Germany), cyclopentyl methyl ether (CPME) from Sigma Aldrich (Japan), dichloromethane (DCM), heptane and isopropanol all from Merck (Darmstadt, Germany). Mobile phase's additives were ammonium acetate from Sigma Aldrich (Japan), formic acid from Sigma Aldrich (Germany) and ammonia from Merck (Darmstadt, Germany). Ultrapure water was obtained from a Milli-Q Purification unit from Millipore (Darmstadt, Germany). The API and the impurities used for this study were provided by UCB Pharma.

3. Software

Data acquisition and processing were carried out using Empower 3.3. Microsoft® Excel® was used to process all resulting data and to simulate predicted chromatograms, by adapting the Excel macro developed by Charlene Galea from the Free University of Brussels (VUB) during her doctoral research.

4. Samples preparation

Since a lot of combinations will result from the full factorial screening, stock solutions were prepared by diluting each standard compound in methanol with 10mg/mL concentration for the API (C2) and 2mg/mL for each of the 17 impurities (C1-C17). To this end, one independent stock solution was prepared for each molecule, except for one of them (C4). This impurity was not available in its pure form and was incorporated in an unknown sample with other impurities and has to be identified in its matrix. To ensure complete dissolution, all solutions were sonicated using an ultrasonic bath for 5min and were stored at 4°C.

To identify each impurity, four different mixtures were prepared from the stock solutions. The impurities having the same molecular mass were put in different mixtures. 1mL of API, 1mL of C4 and 50µL of all remaining impurities were dissolved in a volumetric flask of 10mL by following the plan presented in Table 4. All mixtures were diluted using the different injection solvents investigated. The compound concentrations were chosen to be as close as possible to the samples that will be analyzed in routine by this developed method.

Table 4 : Preparation of compound mixtures. Impurities from mixtures 1 to 3 were added to reach a concentration of 0.01mg/mL whereas C4 and its matrix were injected at 2mg/mL.

Mix 1	Mix 2	Mix 3	Mix 4
C3	C1	C7	C4
C6	C2	C2	
C9	C5	C13	
C10	C8	C16	
C12	C11	C17	
C14	C15	C18	

5. Detection

5.1. Detectors selection

One of the great advantages of SFC is its compatibility with multiple detectors such as UV/Vis, PDA (photodiode array), ELS (evaporative light scattering), and MS (mass spectrometry). In this study, two detectors were required for the analysis of brivaracetam and its impurities. A PDA detector was chosen for its sensitivity, capacity to handle high pressures and because the mobile phases used are UV-transparent below the cut-off wavelength. Indeed, CO₂ and methanol have respectively a UV cut-off wavelength of 190nm and 205nm, respectively (Nováková *et al.*, 2014). Below these wavelengths, the solvents absorb all the light resulting in an increased noise level and loss of sensitivity. However, these limits are low and thus allow a broad working range. Also, a second detector was required for impurity identification due to their large number and their great similarity. For these reasons, mass

spectrometry was the most suitable complementary detector due to its sensitivity, capability for high-throughput analysis and for providing structural information.

5.2. Compounds data

The compounds of interest for this study were previously analyzed by HPLC-MS, and their mass data is presented in Table 5. Their exact mass allowed their identification by the MS detector.

Table 5 : MS data of Brivaracetam and its impurities recorded by HPLC-MS.

Number	Exact mass	MH+	MNa+	MK+	Daughter ion 1	Daughter ion 2
C1	126,16	127	-	-	-	-
C2 (API)	212,29	213	235	251	168	-
C3	212,29	213	235	251	168	-
C4	210,27	211	233	249	194	166
C5	210,27	211	233	249	194	166
C6	208,3	209				
C7	142,16	143	-	181	125	-
C8	226,27	227	249	265	182	-
C9	228,29	-	251	267	166	211
C10	224,26	225	247	263	180	-
C11	297,39	298	320	336	168	-
C12	295,38	296	296	-	-	-
C13	228,29	229	251	267	203	184
C14	228,29	229	251	267	184	166
C15	228,29	229	-	-	166	184
C16	211,26	212	234	250	166	-
C17	298,38	299	321	337	168	-

6. Screening of injection solvents, stationary phases and mobile phases

6.1. Full factorial screening methodology

6.1.1. Objective definition

The screening study aims to select the combination of injection solvent, stationary phase and organic modifier that provide the best peak shape and chromatographic efficiency. Because the interactions between these three chromatographic parameters are not negligible, a full factorial design was applied, testing all the combinations.

6.1.2. CQAs definition

The screening experiments were focused on three criteria all influencing the peak shape, which is usually difficult to improve during the optimization phase.

➤ Tailing factor (T_f)

The tailing factor is the coefficient defined by US Pharmacopeia for peak symmetry, calculated by the equation:

$$T_f = \frac{w_{0.05}}{2f} \quad (\text{Eq. 1})$$

Where $w_{0.05}$ is the width of the peak at 5% height and f represents the distance from the peak maximum to the leading edge of the peak, the distance being measured at 5% peak height from the baseline (Fig. 17).

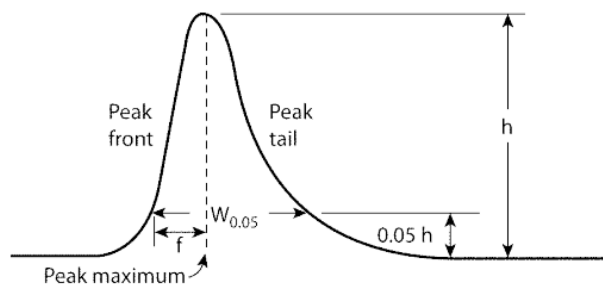


Figure 17: Components used to calculate the tailing factor of an asymmetrical peak (US Pharmacopeia).

A perfectly symmetrical peak would have a T_f value of 1. Smaller values than 1 imply peak fronting whereas higher values indicate peak tailing.

➤ Peak capacity (P_C)

The peak capacity was used in this study to evaluate the performance of a gradient separation (Neue, 2005). The objective is to gain the highest peak capacity, calculated as follows:

$$P_C = 1 + \frac{t_G}{\left(\frac{1}{n}\right) \sum_1^n w} \quad (\text{Eq. 2})$$

Where t_G is the gradient run time, w is the baseline peak width and n is the number of peaks selected for the calculation. Based on the peak width, investigation of P_C provides information about the overall peak sharpness. As low is the baseline peak width and as high would be the P_C .

➤ Peak height (*h*)

Considering the small amount of impurities found in the samples that have to be analyzed by the current method, the peak height was also studied. Indeed, the impurities that have a too low absorbance risk of not being detected if they are involved in too low concentrations. This is avoided by selecting the highest peak height.

6.1.3. Full factorial screening

A total of 72 experiments (6 x 4 x 3) were defined by full factorial design. The experimental plan of screening design is described in Fig.18. Considering the quite good solubility of the compounds in organic solvent, six of the commonly used injection solvents were chosen for this screening study (Abrahamsson and Sandahl, 2013; Desfontaine *et al.*, 2017). The columns were selected to have a wide range of polarities (Berger, 2015) with a particular focus on reduced particle size (maximum 2µm) for maximal efficiency. Regarding the mobile phase choice, using water as an additive was proven to drastically improve peak shapes (West, 2013). For this reason, 2% of water as additive was included in every mobile phase tested. Ammonium acetate and formic acid were tested as additives since they are well recommended for pharmaceuticals analysis (Alexander *et al.*, 2013; De Klerck, Vander Heyden and Manglings, 2013). However, the use of organic additive is not always required for good peak shape. The combination of acetonitrile with a polar alcohol has been found to increase retention time and to improve selectivity (Nováková *et al.*, 2014; Muscat Galea, Mangelings and Vander Heyden, 2017). Therefore, a mixture of methanol and acetonitrile (50/50 v/v) was also investigated.

Injection solvents		Stationary phases		Mobile phases
Methanol	X	Waters UPC ² BEH 100 x 3mm id., 1,7 µm	X	MeOH + 2% H ₂ O + 20mM AmAc
MTBE		Waters UPC ² Torus 2-PIC 100 x 3mm id., 1,7 µm		MeOH + 2% H ₂ O + 0,1% FA
CPME		Princeton SFC 2-EP 100 x 3mm id., 1,8 µm		MeOH/ACN (50:50) + 2% H ₂ O
ACN		Waters UPC ² HSS C18 SB 150 x 3mm id., 1,8 µm		
DCM				
Heptane/IPA (90:10)				

Figure 18: Screening design (Part I): Factors and their respective levels.

Some well-established stationary phases such as BEH Silica, 2-ethylpyridine (2-EP) and HSS C18 SB are widely used in SFC analysis (Dispas *et al.*, 2016). It is thus important to test recently launched column ligands and chemistries with the classical ones used to achieve the best conditions for compounds analysis. To evaluate the interest of some new stationary phases, OH5 (HILIC selectivity), Diol, and 1-AA chemistries were also screened for the method development (Fig. 19). Due to time and instrumental limitations, they were only tested with MTBE as injection solvent and methanol

combined with 2% of water as mobile phase additive. This choice will be discussed in the results section.

Injection solvent		Stationary phase		Mobile phase
MTBE	X	Supelco Ascentis Express OH5 100 x 2.1mm id., 2µm	X	MeOH + 2% H ₂ O
		Waters UPC ² Torus Diol 100 x 3.0mm id., 1.7µm		
		Waters UPC ² Torus 1-AA 100 x 3.0mm id., 1.7µm		

Figure 19: Screening design (Part II): different new columns are tested with the optimal parameters of injection solvents and mobile phases selected from the first step.

6.2. Screening chromatographic conditions

A generic method was used to perform all screening experiments. A constant flow rate was set at 1.0mL/min for the column Acquity UPC² HSS C18 SB (Fig. 20), at 1.3mL/min for the three first screened columns (Fig. 21) and at 1.2 mL/min for the three remaining columns (Fig. 22). Gradient elution is described in the same respective figures. Temperature was kept at 40°C and backpressure at 150bar. The pressure has to be monitored in compliance with instrumental limits of the chromatographic system, for which the maximum flow rate and pressure are limited to 4mL/min and 413 bars respectively (Nováková et al., 2014). The injection volume was 5µL and the measured dwell volume was 440µL. Chromatograms were recorded at 205nm, which was a compromise between the maximum absorbance of brivaracetam and the cut-off point of methanol. The make-up flow was composed of a mixture of methanol and acetonitrile (80/20: v/v) with 0.1% formic acid, and the cone voltage was set at 10 V.

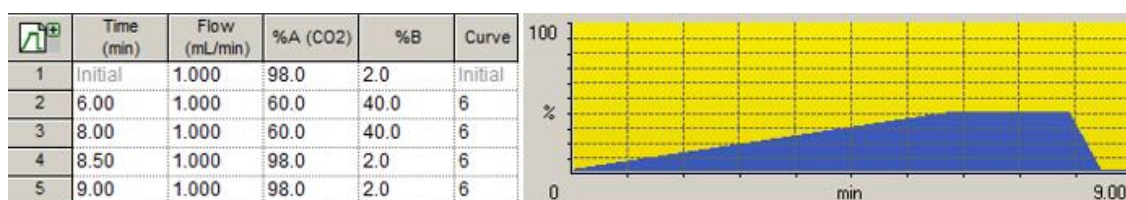


Figure 20: Chromatographic conditions for Acquity UPC² HSS C18 SB. Time, flow rate and gradient composition are presented in the left part. A graphical representation of the percentage of modifier (methanol) is represented as a function of the run time, is shown on the right.

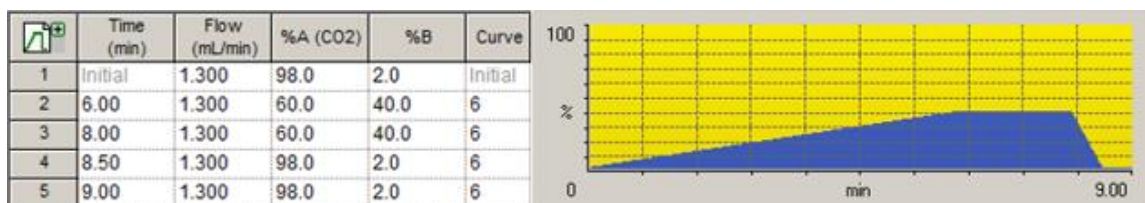


Figure 21: Chromatographic conditions for Acquity UPC² BEH, Acquity UPC² Torus 2-Pic and SFC 2-Ethylpyridine. Time, flow rate and gradient composition are presented in the left part. A graphical representation of the percentage of modifier (methanol) is represented as a function of the run time, is shown on the right.

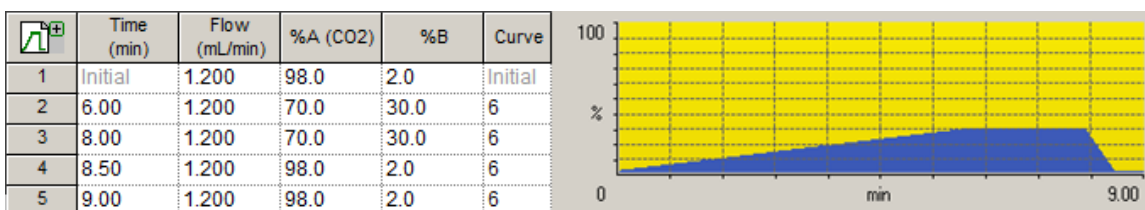


Figure 22: Chromatographic conditions for Acquity UPC² Torus 1-AA, UPC² Torus Diol and Supelco Ascentis Express OH-5. Time, flow rate and gradient composition are presented in the left part. A graphical representation of the percentage of modifier (methanol) is represented as a function of the run time, is shown on the right.

7. Method optimization

7.1. Objective definition

In this part the optimal analytical chromatographic conditions, for which all compounds of a mixture containing brivaracetam and its impurities are separated, are searched. This is achieved by applying DoE methodology and RSM design.

7.2. Selection of the analytical chromatographic parameters

The parameters to be optimized constitute the independent variables of the model. Their choice depends on how their impact SFC and the analytes. Their respective levels are usually built from the conditions identified during the screening, namely control.

The backpressure and the temperature are good candidates since they both have significant effects on CO₂ density which results in retention time's variation. However, compound 7 is thermally unstable and the temperature range was really small for optimization. On the other hand, it was previously demonstrated that peak shape was significantly improved when increasing the percentage of H₂O and this up to 10% (West, 2013). Therefore, higher percentages of water (than 2%) were investigated. Last but not least, gradient time could influence retention time and should be as short as possible but at the same time, long enough to obtain an efficient separation. The independent variables and their levels are summarized in Table 6. The other parameters were kept constant during the experimental design.

Table 6 : The 3 chromatographic DoE parameters selected for method optimization. For each factor, three levels were investigated.

Factors	-1	0	1	Control
%H2O	2	4	6	2
BP (bar)	120	150	180	150
BP (psi)	1740	150	2611	150
Gradient time (min)	5	6	7	6

7.3. Model responses and CQAs definition

Determination of the optimal analytical chromatographic conditions can rely on the evaluation of two CQAs: the chromatographic resolution (R_s) and separation criterion (S).

7.3.1. The chromatographic resolution (R_s)

R_s is used to evaluate the separation of two peaks and directly depends on the retention time, the peak width, and indirectly on the peak height and the asymmetry factor. However, the resolution cannot be selected as direct response of the model since prediction of the model can lead to inversion of peaks and would therefore skew the results. To prevent peak inversion in model prediction, this study suggests using the retention times and the peaks width at half height as responses of the models based on which, the CQA, R_s between peak a and peak b respectively (Fig. 22), is thereafter calculated as follows:

$$R_s = \frac{1.18 \times (RT_b - RT_a)}{(w_{0.5a} + w_{0.5b})} \quad (\text{Eq. 3})$$

Where RT is the retention time and $w_{0.5}$ is the peak width at half height of the peak.

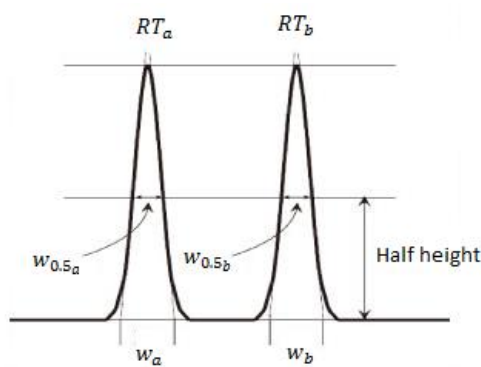


Figure 23: Factors used to calculate the resolution between peak a and b: w represents the baseline peak widths, RT are the retention times and $w_{0.5}$ are the peak widths at half height.

As a rule of thumbs, a good separation is obtained for a R_s value ≥ 1.5 between two impurities and a R_s value ≥ 2.0 between the API and the first impurity eluting before or after it.

7.3.2. The Separation criterion (S)

Another separation criterion (S) has been recently proposed (Debrus *et al.*, 2011; Rafamantanana *et al.*, 2012; Andri *et al.*, 2017). The S criterion is defined as the difference between the beginning of a second peak and the end of the first one (Fig. 22). Peak start and peak end retention times for each peaks were defined as the model responses, based on which the CQA, S is thereafter calculated as follows:

$$S = RT_{start_b} - RT_{end_a} \quad (\text{Eq. 4})$$

The peaks are baseline-resolved if $S \geq 0$.

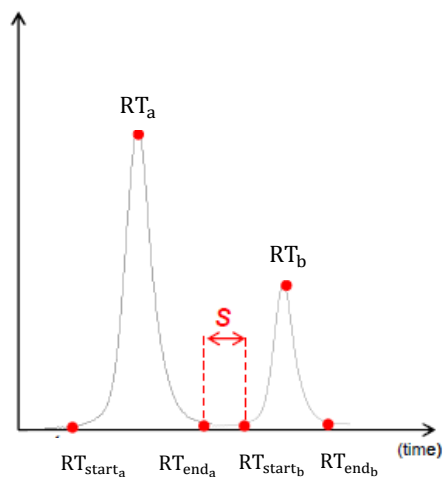


Figure 24: Separation factor between peak a and peak b ((Rafamantanana *et al.*, 2012)

7.4. Chromatographic conditions of optimization

The chromatographic parameters settings are summarized in Table 8 and gradient elution applied in DoE are detailed in Table 9. The choice of a mobile phase composed of maximum 30% of organic phase was made in compliance with the green interest of SFC.

Table 7: Chromatographic parameters setting of Waters UPC² SFC system for optimization analysis

Modules	Parameters setting
Binary Solvent Manager (BSM)	Mobile phase A: CO ₂ Mobile phase B: MeOH + 2% H ₂ O Flow rate: 1.2mL/min Seal wash: MeOH
Sample Manager (SM)	Injection solvent : CPME Injection volume: 5μL Sample temperature: 4°C Strong wash: MeOH Weak wash: MeOH/ACN (50/50 v/v)
Column Manager (CM)	Column chemistry: Waters UPC ² Torus 1-aminoanthracene Column dimensions: 100 x 3mm id., 1.7μm Temperature: 40°C
Photodiode Array detector (PDA)	λ= 105nm Resolution: 1.2 nm Sampling rate: 20points/sec
Convergence Manager (CCM)	Back-pressure regulator: 150 bar (150 psi)
ISM and QDa	Make-up flow composition: MeOH/H ₂ O (80/20 v/v) + 0.1% FA Make-up flow rate: 0.39 mL/min Cone voltage: 10 volts Capillary voltage: 1.2 kV (positive), 0.8kV (negative) Sampling rate: 10points/sec

Table 8: Gradient times t_G tested and related mobile phase compositions in DoE analysis

t_{G_5} (min)	t_{G_6} (min)	t_{G_7} (min)	Mobile phase A (%) CO ₂	Mobile phase B (%) MeOH +2% H ₂ O
0	0	0	98	2
5	6	7	70	30
7	8	9	70	30
7.5	8.5	9.5	98	2
8	9	10	98	2

7.4.1. Design creation

Once the objectives and factors are defined, the experimental domain to be explored is shaped using the face-centered central composite (CCC) design (Fig 23). This design is based on a response surface model. The experiments were performed according to the related experimental plan, presented in Table 7.

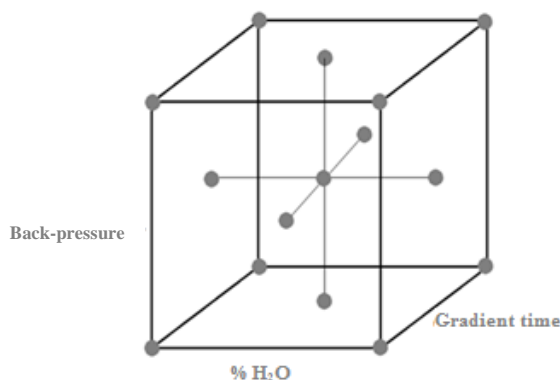


Figure 25: Experimental domain resulting from the investigation of the backpressure, the percentage of water as additive and the gradient time using the face-centered central composite design.

Table 9 : Face-centered central composite experimental design used in this study includes 15 experiments and 4 controls. The design contributes to the optimization of 3 analytical chromatographic parameters: the percentage of H₂O as additive in the mobile phase, the back-pressure and the gradient time.

Experiment number	% H ₂ O	Back-pressure (bar)	Gradient time (min)
Control1	2	150	6
13	4	150	7
5	2	180	5
3	6	120	5
11	6	150	6
6	6	180	5
Control2	2	150	6
10	2	150	6
12	4	150	5
8	6	180	7
1	2	120	5
14	4	120	6
Control3	2	150	6
7	2	180	7
4	6	120	7
2	2	120	7
15	4	180	6
9	4	150	6
Control4	2	150	6

7.4.2. Model creation

On the basis of the 15 run experiments presented in Table 9, the measured variables illustrated in Fig.24 were extracted from the respective UV chromatograms for each compound.

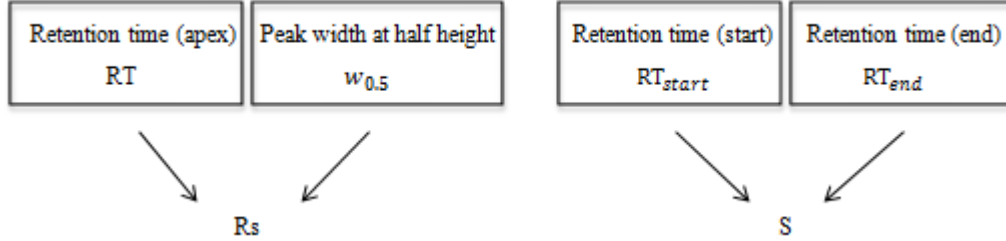


Figure 26: Extraction of variables: the retention time at apex (RT), the peak width at half height ($w_{0.5}$), the retention time at the beginning (RT_{start}), and at the end (RT_{end}) based on which the corresponding CQA: resolution (Rs) and separation (S) are calculated respectively.

Based on the RSM design, predictive models are then built for each variable (RT, $w_{0.5}$, RT_{START} and RT_{end}) and each compound. The corresponding polynomial functions, each describing the effects between the response and the chromatographic parameters, are described as follows:

$$RT = b_0 + b_1 \cdot \%H_2O + b_2 \cdot BP + b_3 \cdot GT + b_{11} \cdot \%H_2O^2 + b_{22} \cdot BP^2 + b_{33} \cdot GT^2 + b_{12} \cdot \%H_2O \cdot BP + b_{13} \cdot \%H_2O \cdot GT + b_{23} \cdot BP \cdot GT + b_{123} \cdot \%H_2O \cdot BP \cdot GT + \epsilon$$

$$w_{0.5} = b_0 + b_1 \cdot \%H_2O + b_2 \cdot BP + b_3 \cdot GT + b_{11} \cdot \%H_2O^2 + b_{22} \cdot BP^2 + b_{33} \cdot GT^2 + b_{12} \cdot \%H_2O \cdot BP + b_{13} \cdot \%H_2O \cdot GT + b_{23} \cdot BP \cdot GT + b_{123} \cdot \%H_2O \cdot BP \cdot GT + \epsilon$$

$$RT_{START} = b_0 + b_1 \cdot \%H_2O + b_2 \cdot BP + b_3 \cdot GT + b_{11} \cdot \%H_2O^2 + b_{22} \cdot BP^2 + b_{33} \cdot GT^2 + b_{12} \cdot \%H_2O \cdot BP + b_{13} \cdot \%H_2O \cdot GT + b_{23} \cdot BP \cdot GT + b_{123} \cdot \%H_2O \cdot BP \cdot GT + \epsilon$$

$$RT_{end} = b_0 + b_1 \cdot \%H_2O + b_2 \cdot BP + b_3 \cdot GT + b_{11} \cdot \%H_2O^2 + b_{22} \cdot BP^2 + b_{33} \cdot GT^2 + b_{12} \cdot \%H_2O \cdot BP + b_{13} \cdot \%H_2O \cdot GT + b_{23} \cdot BP \cdot GT + b_{123} \cdot \%H_2O \cdot BP \cdot GT + \epsilon$$

Where RT, $w_{0.5}$, RT_{START} and RT_{end} are the model responses, b the regression coefficients, and ϵ corresponds to the residual or the model error and $\%H_2O$, BP and GT constitute the chromatographic parameters to be optimized or also namely, the explicative variables of the model. The predictive models investigate the main effects (first-order terms in red), the quadratic and factor interactions (second-order terms in blue and green respectively). The model quality was examined by Analysis of Variance (ANOVA), R^2_{adj} analysis and residuals distribution investigation.

The model was thereafter used for prediction of responses (RT , $w_{0.5}$, RT_{START} and RT_{end}). Regression coefficients and residuals were determined by the least squares regression calculations. Hence, the responses were computed for every compound and over the entire experimental domain. Indeed, the level range initially investigated for each factor was split in 6 levels (-1; -0.6; -0.2; 0.2; 0.6; 1) and all combinations of these factor-levels were investigated. In other words, the experimental domain was split into 216 points representing smaller areas in each of which, the separation ability was investigated. For this purpose, the responses were then sorted by retention times in compliance with the peak elution order, representing the simulated composite chromatogram.

Finally, both resolution and S factor were calculated to evaluate the separation of each pair of consecutive peaks. The minimal Rs and minimal S are compared by using response surface plots. T

V. Results and discussion

1. Screening of injection solvents, stationary phases and mobile phases

1.1. Full factorial design

In the screening study, the objective was to obtain the best peak shape. Complete baseline separation of the compounds did not constitute the main goal. Therefore, resolution criterion is not involved in this part and results are discussed according to the critical quality attributes (CQAs) previously mentioned; i.e. tailing factor (T_f), peak capacity (P_C) and peak height (h). An overlay of all chromatograms was also visually analyzed to confirm the results. Moreover, only the Mix 1, 2 and 3 were discussed in this part. The mixture 4 contains a lot of unknown impurities. Therefore, it is difficult to evaluate the chromatogram quality since only C4 is of interest. The best combination of injection solvent, stationary and mobile phase was first defined then the identification and evaluation of C4 peak was thereafter achieved.

Considering the large number of experiments and compounds investigated, some conditions were not satisfactory due to peak co-elutions. Therefore, it was sometimes impossible to extract the peak width of all compounds. Moreover, processing the data by taking into account the mean tailing factor for all compounds might skew the results. Indeed, if half of the peaks included fronting and the remaining half showed tailing, then the resulting mean T_f would be around 1. For these reasons, brivaracetam, which was eluted using all screening combinations, was chosen to study the T_f , the P_C and h .

1.1.1. Injection solvent selection

As current practice, it is recommended to dissolve the sample in a solvent having similar elution strength to the mobile phase composition at the injection, in order to minimize peak distortion. Thus, the non-polar diluents should be of high interest. The effect of injection solvent on tailing factor and peak capacity considering different columns, according to each mobile phase tested is illustrated in Fig. 26. The superiority of non-polar solvents such as heptane/IPA and MTBE is not obvious compared to the expectations. Acetonitrile which has polar property enabled to improve peak shape

for the BEH and HSS C18 SC columns compared to heptane/IPA mixture. On the other hand and as previously demonstrated by other studies (Abrahamsson and Sandahl, 2013; Desfontaine *et al.*, 2017), the use of MeOH showed the worst peak shapes for all stationary and mobile phases combinations. From the T_f point of view, MTBE and CPME globally exhibit peak tailing while the remaining injection solvents display peak fronting.

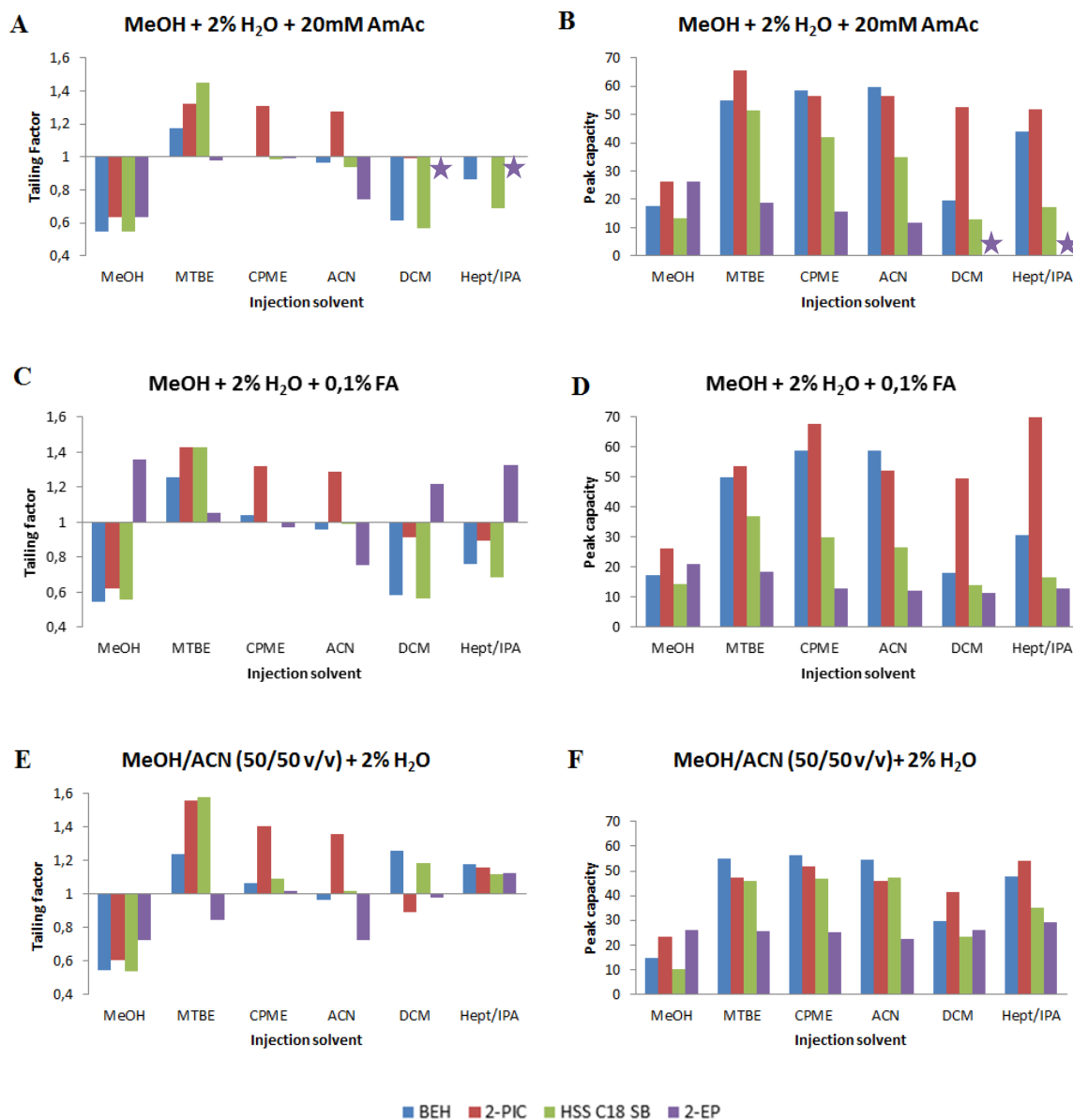


Figure 27: Effect of injection solvents on brivaracetam peak shape (tailing factor and peak capacity) when considering different stationary and mobile phases. The columns tested involve BEH silica (in blue), 2-PIC (in red), HSS C18 SB (in green) and 2-EP (in purple) chemistries. Tailing factor of brivaracetam when considering the mobile phases: (A) MeOH + 2% H₂O + 20mM AmAc, (C) MeOH + 2% H₂O + 0.1%FA and (E) MeOH/ACN (50/50 v/v) + 2% H₂O. Peak capacity of brivaracetam when considering the mobile phases: (B) MeOH + 2% H₂O + 20mM AmAc, (D) MeOH + 2% H₂O + 0.1%FA and (F) MeOH/ACN (50/50 v/v) + 2% H₂O. The purple stars represent the 2 conditions that were not tested due to instrumental limitations.

Another parameter that should not be overlooked is the peak height, which is related to the absorbance capacity. Indeed, a high peak height is preferred to make sure that the developed method will contribute to the best peak shapes for impurities which might be present in very small amounts. The effect of injection solvents on peak height when considering all combinations of columns and mobile phase is illustrated in Fig. 27. The worst injection solvent (MeOH) and column (2-EP) are confirmed respectively. Regarding the aprotic solvents, they did not show a different impact on the 2-PIC column and their resulting absorbance was all acceptable. The use of MTBE, CPME and ACN provided the highest peak height for BEH, 2-PIC and HSS C18 SB.

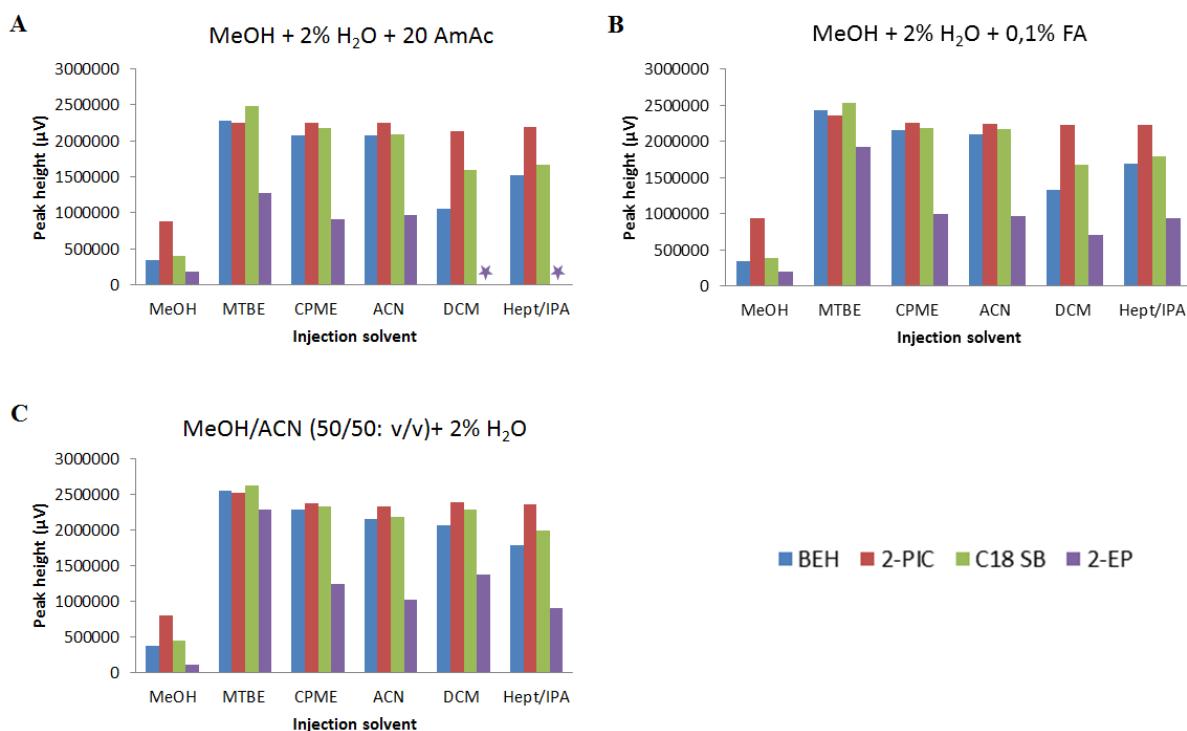


Figure 28: Effect of injection solvent on brivaracetam on absorbance (peak height) when considering different stationary and mobile phases. The columns tested involve BEH silica (in blue), 2-PIC (in red), HSS C18 SB (in green) and 2-EP (in purple) chemistries. Peak height of brivaracetam when considering the mobile phases: (A) MeOH + 2% H₂O + 20mM AmAc, (B) MeOH + 2% H₂O + 0.1% FA and (C) MeOH/ACN (50/50: v/v) + 2% H₂O. The purple stars represent the 2 conditions that were not tested due to instrumental limitations.

The effect of injection solvent on Mix 1 when considering a mixture of MeOH/ACN (50/50: v/v) + 2% H₂O as mobile phase and HSS C18 SB as stationary phase is illustrated in Fig. 28. As depicted in this figure, MTBE provided the best peak shape. DCM showed a good absorbance but broader peaks. Heptane/IPA (90:10: v/v) and CPME presented quite similar sharp peaks. The latter had the advantage to provide the least peak tailing for most of the columns but slightly poorer peak capacities. It is important to notice that this result is in contract with the high tailing factor for brivaracetam using MTBE as injection solvent (Fig. 26E). However, as the goal is to obtain the best separation of the drug and all its impurities, conditions leading to the best peak shape for the impurities were preferred.

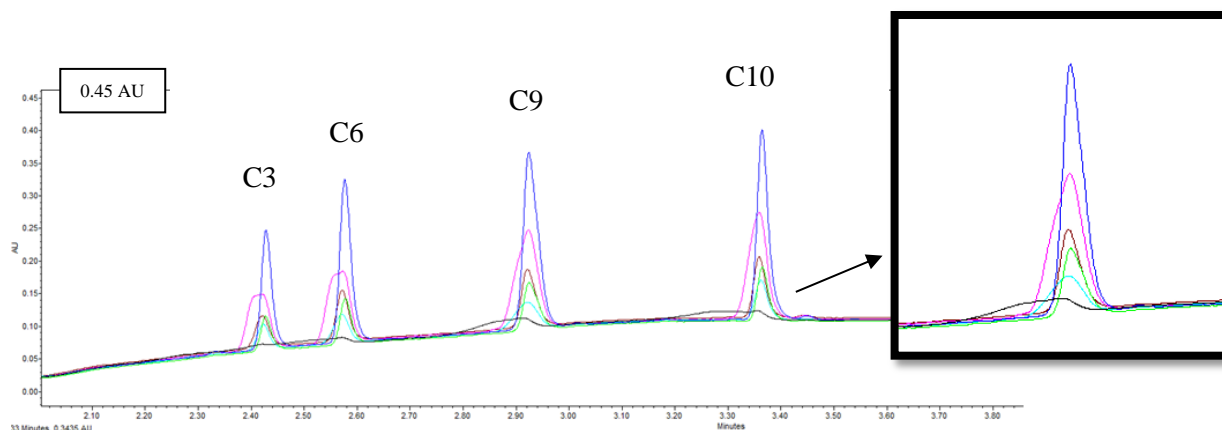


Figure 29: Effect of injection solvents on column HSS C18 SB when considering a mixture of MeOH/ACN (50/50: v/v) +2% H₂O for Mix 1 containing C3- C6-C9-C10-C12-C14. The UV chromatogram presents the following diluent solvents: MTBE in dark blue), DCM (in pink), heptane/IPA (90/10: v/v) (in brown), CPME (in green), ACN (in turquoise blue) and methanol (in black).The Y-axis represents the absorbance unit and the X-axis shows the run time in minutes.

1.1.2. Mobile phase selection

In the context of pharmaceutical analysis, the use of organic additive was demonstrated to significantly improve the peak shape (Alexander *et al.*, 2013; Nováková *et al.*, 2014; Desfontaine, Veuthey and Guillarme, 2016). The effect of mobile phase composition on tailing factor, peak capacity and peak height of brivaracetam, when considering different columns and MTBE as injection solvent is presented in Figs. 29A- 29C respectively. The interest of AmAc and FA was observed to reduce the tailing factor. However, it was almost always not the case when considering peak capacity and peak height.

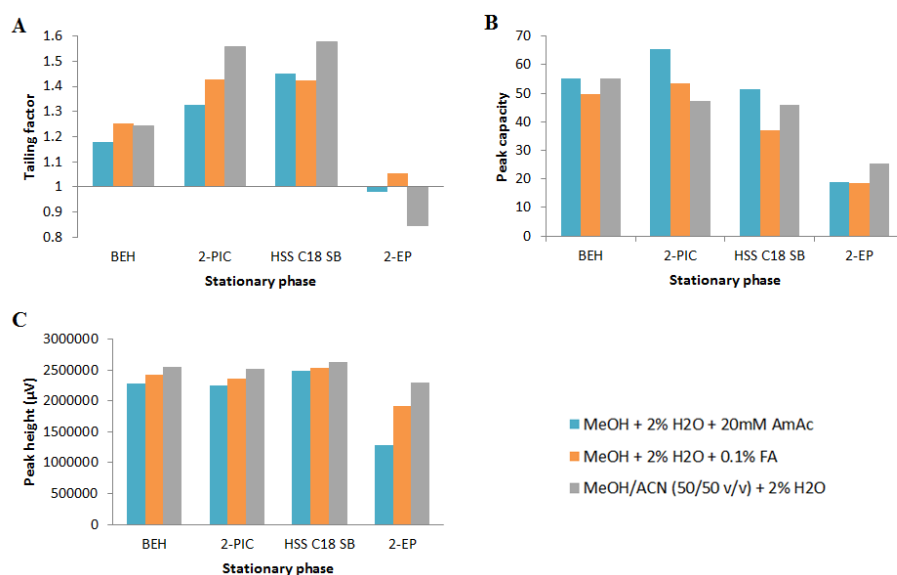


Figure 30: Effect of mobile phases on brivaracetam on peak shape (A) tailing factor, (B) peak capacity and (C) peak height when considering MTBE as injection solvent and the following stationary phases: BEH silica, 2-PIC, HSS C18 SB and 2-EP. Comparison was made between the following mobile phases: MeOH + 2% H₂O + 20mM AmAc (in blue), MeOH + 2% H₂O + 0.1% FA (in orange) and MeOH/ACN (50/50: v/v) + 2% H₂O (in grey).

Indeed, the mobile phase containing no organic additive has shown better absorbance as reflected in the peak height. In fact the compounds analyzed in this study were quite polar and therefore did not always require the use of an organic additive (Berger, 2015). Moreover, their presence has been observed to increase the baseline noise (Fig. 30). Since the advantages of AmAc and FA for improving peak shape was not obviously demonstrated, the choice of avoiding organic additive is preferred for developing a method as green as possible, and this in compliance of the green interest of SFC.

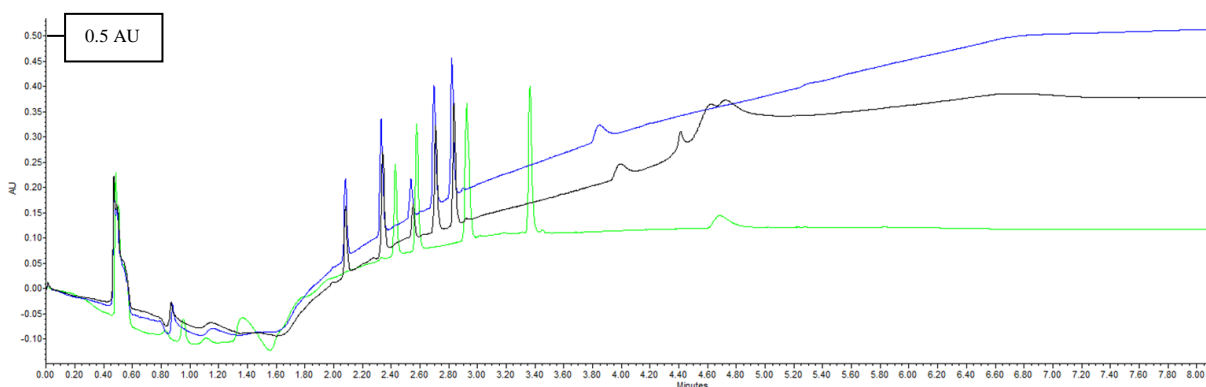


Figure 31: Chromatograms obtained for Mix 1 using different mobile phases (on column HSS C18 SB and MTBE as injection solvent): MeOH + 2% H₂O + 0.1% FA (in blue), MeOH + 2% H₂O + 20mM AmAc (in black) and MeOH/ACN (50/50: v/v) + 2% H₂O (in green). The Y-axis represents the absorbance unit and the X-axis shows the run time in minutes.

1.1.3. Column selection

From Fig. 27, some conclusions may be already drawn regarding the effect of stationary phases on the peak shape. On the whole, the use of 2-ethylpyridine (2-EP) stationary phase (in purple) presented the poorest peak capacities. However, BEH silica (BEH) (in blue) and 2-picolylamine (2-PIC) (in red) chemistries both exposed sharper peaks. The elution profile of mix 2 when considering MTBE as diluent solvent, MeOH/ACN (50/50 v/v) + 2% H₂O as mobile phase and the 4 tested columns is illustrated in Fig. 31. HSS C18 SB was observed to show the best compromise between peak capacity, symmetry of peak and UV absorbance.

Large differences were observed between retention of the compounds on the four stationary phases. Globally, 2-PIC had slightly higher retention (2.6min) compared to the BEH (1.9 min) and HSS C18 SB (2.35 min) columns regardless the conditions (Fig. 31). This is maybe due to the presence of aromatic interactions of compounds with 2-PIC whereas BEH and HSS C18 SB are free of aromatic rings on the ligand. Despite the fact that the 2-EP stationary phase is in general providing the best peak shape in SFC, this column showed the poorest peak shape and retention for the compounds included in this study and this, regardless the conditions.

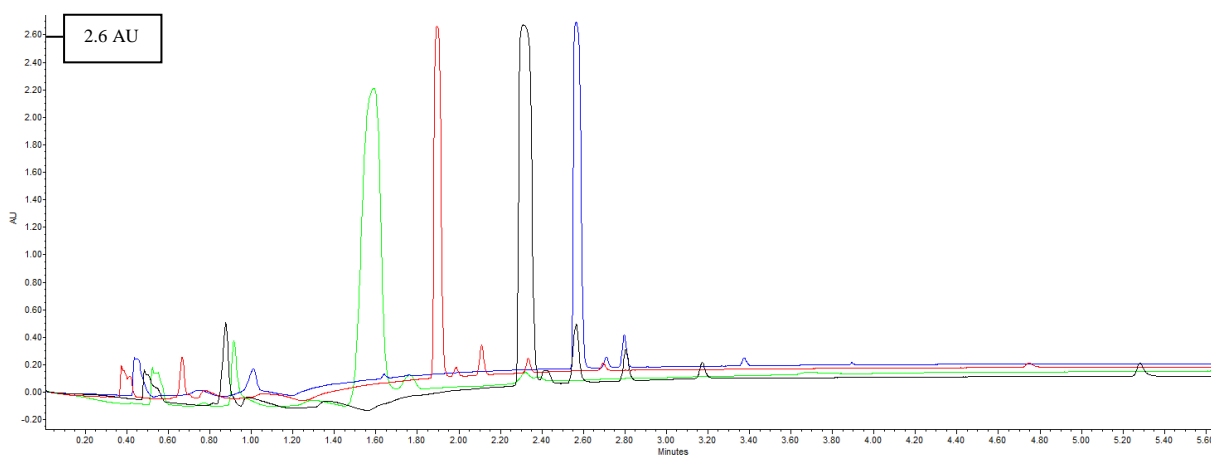


Figure 32: Chromatograms of Mix2 when considering MTBE as injection solvent and MeOH/ACN (50/50:v/v) +2% H₂O as mobile phase and different stationary phases: 2-EP (in green), BEH silica (in red), HSS C18 SB (in black) and 2-PIC (in blue).

1.2. Screening of alternative stationary phases

The best injection solvent (MTBE) was considered to investigate some additional stationary phase chemistries. Regarding the mobile phase, the use of organic additive was not recommended for this study. The use of acetonitrile in the mobile phase was investigated in the beginning because it is known to increase compounds retention. Since a lot of compounds are involved in this study, acetonitrile properties used in the mobile phase could provide an improved separation. However and in compliance with the green interest of SFC, the objective was to use as less as possible harmful organic solvent. In this context, the use of acetonitrile in the mobile phase was avoided since it is more toxic (and more expensive) than methanol. Therefore, the mobile phase that was considered for columns screening was MeOH with 2% H₂O.

Concerning the results, the elution profile was different for each column tested suggesting the potential orthogonality between the columns. The use of 1-AA stationary phase was observed to show the best peak shape (as a compromise between the three criteria) compared to OH-5 and Diol columns (Fig. 32). Regarding the selectivity, this stationary phase presented higher retention times for the less polar compounds. A strong retention of C1 was observed, which can suggest this column was designed for neutral non-polar compounds (Fig. 33). However, the majority of the compounds analyzed in this study present neutral to polar property which could make OH-5 of interest compared to 1-AA. Indeed, the HILIC OH-5 globally showed good peak shape and acceptable retention times for all compounds except C1. The poor retention of C1 (less than 0.5 min) could not make it a column of choice for this study. Regarding the Diol ligand, similar observation was made, an intermediate but still poor retention time (less than 0.8 min) for C1 was observed which justifies its exclusion.

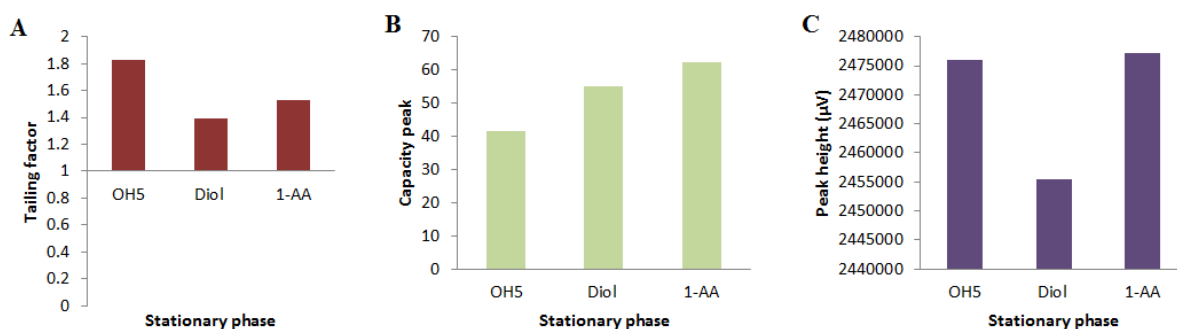


Figure 33: Effect of stationary phase on brivaracetam peak shape (with MTBE as injection solvent and MeOH + 2% H₂O as mobile phase): OH-5, Diol and 1-AA. (A) Tailing factor in red (B) Capacity peak in green (C) Peak height in purple are the criteria based on which the peak shape is characterized.

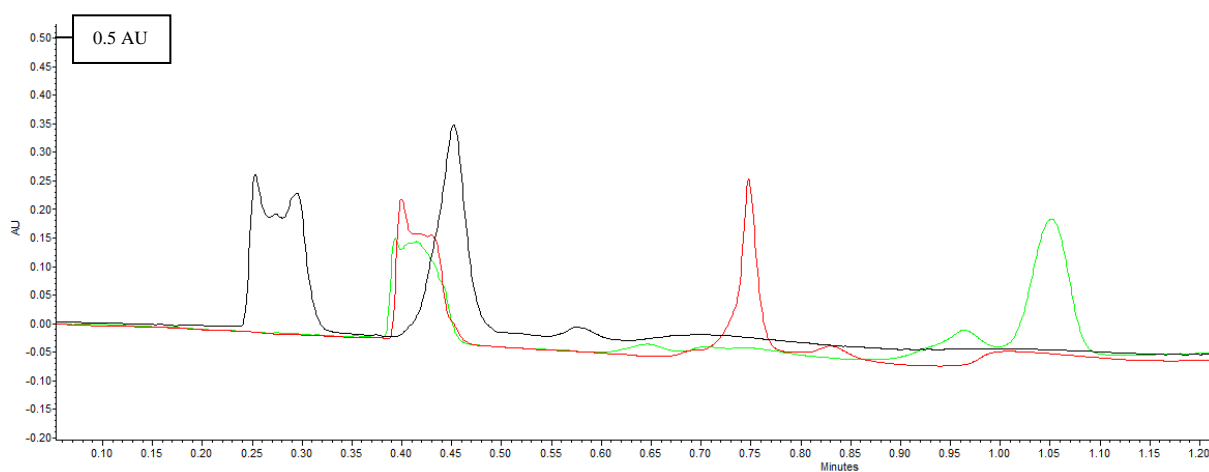


Figure 34: Chromatograms of Cl when considering MTBE as injection solvent, MeOH +2% H₂O as mobile phase and different column ligands: OH-5 (in black), Diol (in red) and 1-AA (in green).

In the end, some conclusions can be drawn when considering all columns tested in the framework of this study. As previously mentioned, the chromatograms obtained on 2-EP stationary phase were unacceptable compared to the other columns and this, regardless of the mobile phase or injection solvent selected. HSS C18 SB, which was selected as the best column from the first part of screening study, generated too much pressure in the system and could not be used for the next experiments. Indeed, the pressure was too close to the instrumental pressure limit which is set at 414 bar leading to the system shut down. Thus, the unstable pressure generated could not make it a column of choice. BEH, 2-PIC and 1-AA are all good columns candidates for the compounds being analyzed in this study. The elution profile of Mix 2 for these 3 columns is presented in the Fig. 34. The chromatograms obtained are all acceptable in term of peak shapes. The choice was then made on the retention

selectivity of the first compound eluted. 1-AA allows the highest retention for C1 avoiding its elution in the peak solvent for a future analysis and is therefore the column chosen for the optimization study.

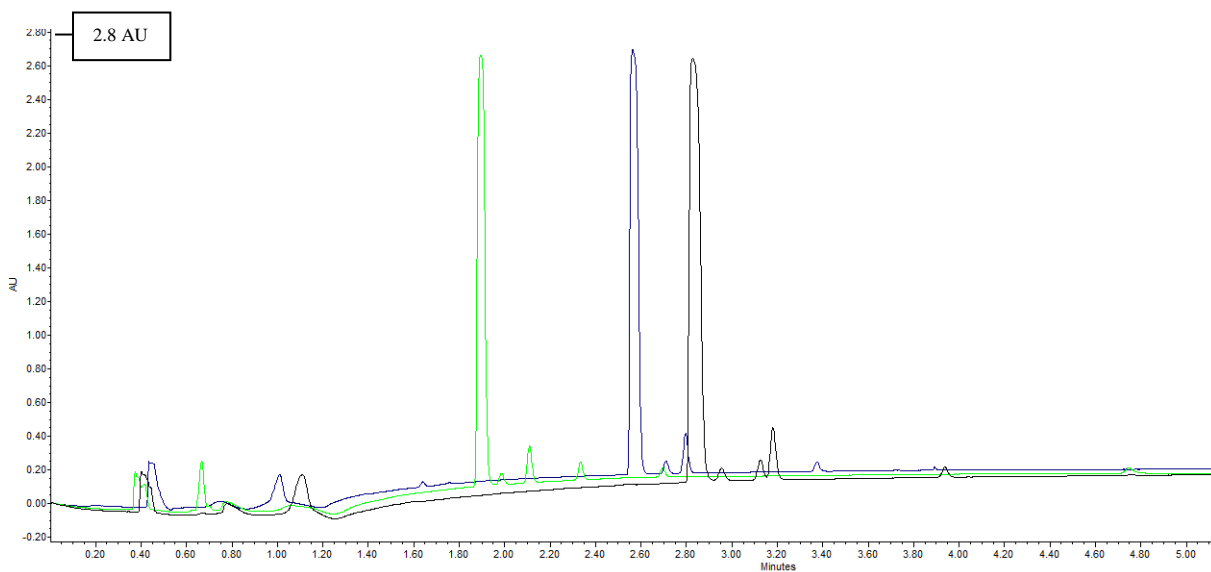


Figure 35: Chromatograms of Mix 2 when considering MTBE as injection solvent, MeOH +2% H₂O as mobile phase and different columns: BEH (in green), 2-PIC (in blue) and 1-AA (in black).

1.3. Resulting screening chromatographic conditions and compounds identification

The best combination of injection solvent, mobile and stationary phase was found to be : MTBE, MeOH+ 2% H₂O and Torus 1-AA respectively (Fig. 35).

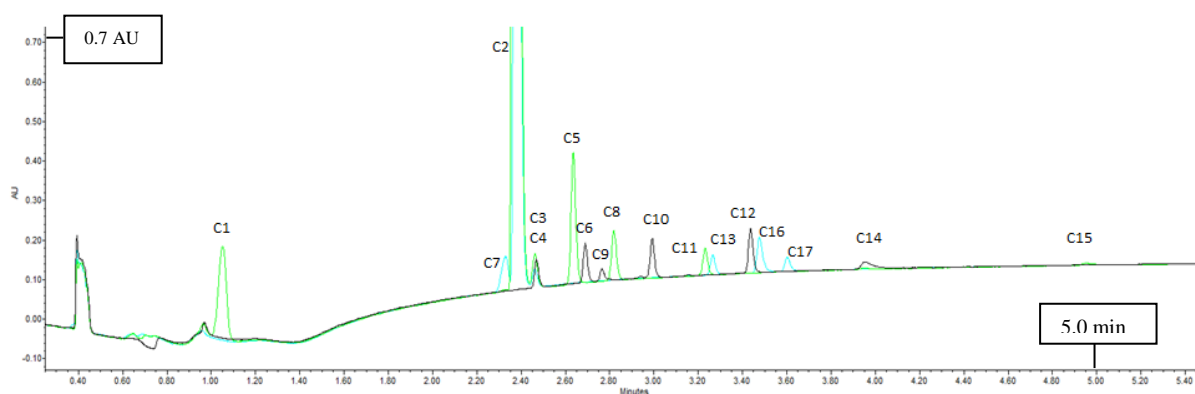


Figure 36: UV chromatogram representing the mixture of brivaracetam and its impurities elution when considering MTBE as solvent injection, MeOH +2% H₂O as mobile phase and 1-AA as stationary phase.

All impurities were identified with the coupled information from the PDA and MS detectors. The isolated compounds from Mix 1 to Mix 3 were easily identified by analyzing their specific masses. Regarding the complex sample which contained C4, the investigation of its typical mass ions revealed its coelution with C3 for almost all the combinations. Since C4 and C5 are isomers and C2 and C3 are diastereoisomers, they produced the same daughter ions respectively. The overlay of the TIC (total Ion Current) plot which shows all masses and the specific daughter ions of C4 and C3 confirmed their coelution. Therefore, this molecule was excluded from the sample. The QDa chromatogram is presented in Fig. 36.

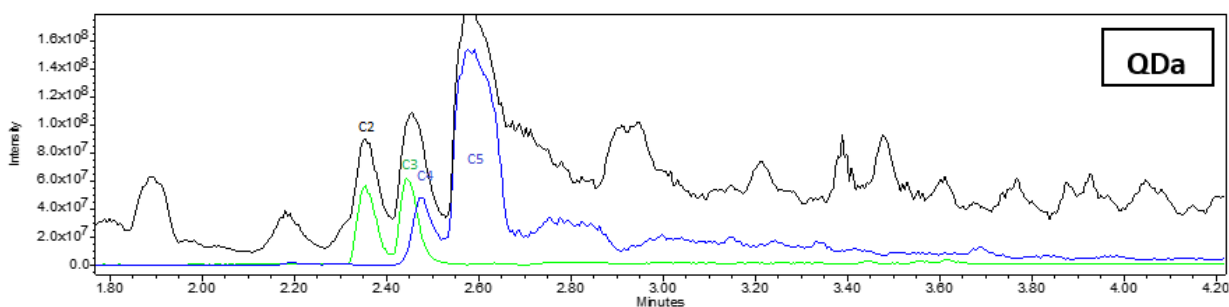


Figure 37: Chromatogram of Mix 4 obtained from QDa detector. Identification of compound number 4 by overlay of TIC (Total Ion Current) plot (in black) and the specific masses of C4 and C5 (in blue). The green trend confirms the coelution of C3 and C4.

Although MTBE gave the best peak shapes for almost all combinations, this organic solvent is toxic and volatile. On the other hand, CPME previously showed good peak shapes but has the advantage to be greener and less volatile. Therefore, this solvent could be a good alternative for future analyzes.

2. Method optimization

The first step consisted of verifying the quality of experiments and created models. Control experiments were performed during DoE and were investigated. A total of 64 models (4 responses x 16 compounds) were computed, testing 216 conditions over the experimental domain. Model validation was achieved by comparing the predicted responses with the experimentally obtained variables from the DoE and by evaluating the adjusted determination coefficients (R^2_{adj}), p-values from ANOVA and normal residuals distribution. Rs and S criteria were computed based on the modeled responses RT , $w_{0.5}$, RT_{start} and RT_{end} . The minimal Rs, the minimal S and the number of coeluted peaks were discussed, leading to the optimal %H₂O, BP and t_G determination. The resulting optimized separation method was then highlighted and experimentally confirmed. Simulation of the predicted chromatograms was achieved using Excel®. Finally the prediction robustness was investigated by fractional factorial design.

2.1. Experiments and model validation

2.1.1. Control experiments

Four replicates of the control condition were carried out during DoE experiments to monitor system and column stability. Moreover and in the context of method optimization, reproducibility can be represented by the control relative standard deviation (RSD), which limit value is typically set at $\leq 2\%$ (Tiwari and Tiwari, 2010). The RSD for each response and each compound are summarized in Table 12.

Table 10 : Relative standard deviation (RSD) expressed in percentage for each compound (C1-C3; C5-C17) and each variable measured from the DoE; retention time (RT), peak width at half height ($w_{0.5}$), retention time at the beginning of the peak (RT_{start}) and at the end of the peak (RT_{end}).

Compounds	RSD (%) of control experiments			
	RT	$w_{0.5}$	RT_{start}	RT_{end}
C1	0.13	2.60	0.16	0.34
C2	0.04	0.43	0.02	0.02
C3	0.05	2.46	0.11	0.11
C5	0.04	0.39	0.05	0.02
C6	0.06	1.00	0.08	0.16
C7	0.02	2.52	0.25	0.02
C8	0.02	1.32	0.06	0.09
C9	0.06	1.87	0.14	0.30
C10	0.07	1.66	0.14	0.09
C11	0.00	1.12	0.10	0.04
C12	0.06	0.37	0.03	0.11
C13	0.05	1.25	0.06	0.09
C14	0.17	6.30	0.05	0.19
C15	0.05	1.94	0.06	0.12
C16	0.15	1.49	0.15	0.09
C17	0.15	0.62	0.18	0.23

The measured $RSD_{w_{0.5}}$ for C1, C3, C7 and C14 were observed to be superior to 2% while all other values were acceptable. As depicted in Fig. 35 which presenting the resulting chromatogram of screening study, C14 always showed a large peak width and was eluted in the last minutes of the gradient time. Thus, this peak might be more impacted by the increasing modifier composition which was essentially composed of methanol. C1 was the first compound eluted next to the solvent peak and it was therefore more likely influenced by the increased noise of this area. Thus, the peak could be distorted and $w_{0.5}$ modified. C3 and C7 are the two peaks eluted next to the API, which has huge absorbance and occupied a wide place in the chromatogram. Hence, predominant C2 could impact the

two little peaks width next to it. However, the acceptance criteria for impurities can be less strict and $RSD_{w_{0.5}}$ inferior to 10% was judged admissible in this study.

2.1.2. Modeling

The model quality for each response and each compound was evaluated. One objective was to maximize the adjusted coefficient of determination (R^2_{adj}) which takes into account the number of terms contained in each model, of each compound (Table 13).

Table 11 : Adjusted coefficient of determination (R^2_{adj}) for the four modeled variables of each compound: retention time (RT) and peak width at half height ($w_{0.5}$), retention time at the peak start (RT_{start}) and retention time at the peak end (RT_{end})

Compounds	R^2_{adj}			
	RT	$w_{0.5}$	RT_{start}	RT_{end}
C1	0.990	0.915	0.947	0.893
C2	0.999	0.953	0.999	0.999
C3	0.999	0.980	0.999	0.999
C5	0.999	0.994	0.999	0.999
C6	0.999	0.937	1.000	0.998
C7	0.999	0.924	0.997	0.999
C8	0.999	0.974	0.999	0.999
C9	0.999	0.230	0.999	0.999
C10	0.999	0.987	0.999	0.999
C11	0.999	0.921	0.999	0.999
C12	1.000	0.988	1.000	1.000
C13	1.000	0.945	0.999	1.000
C14	1.000	0.756	0.999	0.996
C15	1.000	0.934	1.000	0.999
C16	1.000	0.958	1.000	1.000
C17	1.000	0.909	1.000	0.999
Mean	0.9987	0.8939	0.9958	0.9922

Globally, the values are all high indicating a strong correlation between the responses and the three independent variables: the percentage of water as additive (%H₂O), the backpressure (BP) and the gradient time (t_G). However, the particularly low $R^2_{adj_{w_{0.5}}}$ values for C9 (0.230) and C14 (0.756) suggested that their respective peak width at half height are not impacted by the independent variables investigated. Since all retention times responses showed a significant R^2_{adj} value for these compounds, predictions of C9 and C14 were still carried out.

ANOVA confirmed the tendency observed with the R^2_{adj} . The models that had a p-value <5%, explained better the response than a model composed of only a constant single term, which meant that there was at least one parameter that explained the response. Only the $w_{0.5}$ of C9 and C14 models were not relevant and thus constituted poor model quality.

Table 12: Probability value (p-value) for the F-ratio obtained by ANOVA, for the 64 models investigated (four responses for each compound).

Compounds	ANOVA (p-values)			
	RT	$w_{0.5}$	RT_{start}	RT_{end}
C1	1,2E-04	8,3E-03	3,4E-03	1,3E-02
C2	1,4E-06	2,6E-03	9,0E-07	1,6E-06
C3	8,4E-07	5,2E-04	9,2E-07	5,7E-07
C5	1,9E-06	4,1E-05	2,2E-06	2,6E-06
C6	9,2E-07	4,6E-03	1,9E-07	3,6E-06
C7	1,4E-06	6,7E-03	9,4E-06	9,0E-07
C8	2,0E-06	8,4E-04	2,7E-06	1,9E-06
C9	9,8E-07	3,9E-01	7,3E-07	1,4E-06
C10	1,3E-06	2,3E-04	1,0E-06	1,1E-06
C11	8,1E-07	7,2E-03	1,0E-06	1,3E-06
C12	2,6E-07	1,8E-04	2,0E-07	3,1E-07
C13	2,3E-07	3,5E-03	3,8E-07	1,6E-07
C14	1,9E-07	6,1E-02	1,8E-06	1,7E-05
C15	1,1E-08	5,1E-03	5,6E-08	2,2E-06
C16	1,6E-07	2,1E-03	2,2E-07	4,5E-08
C17	1,2E-07	9,5E-03	1,2E-07	1,4E-07

As presented in Fig. 37A-D, there was globally a strong correlation between experimental responses (RT, $w_{0.5}$, RT_{start} and RT_{end}) and their respective predictions for the 15 points investigated in the DoE. Indeed, C1 was always eluted at 1 min while most of the compounds were eluted between 2 and 6 min. the 15 points. However, the good distribution of residuals (Fig. 37F) allowed accepting the model although its quality was not perfect.

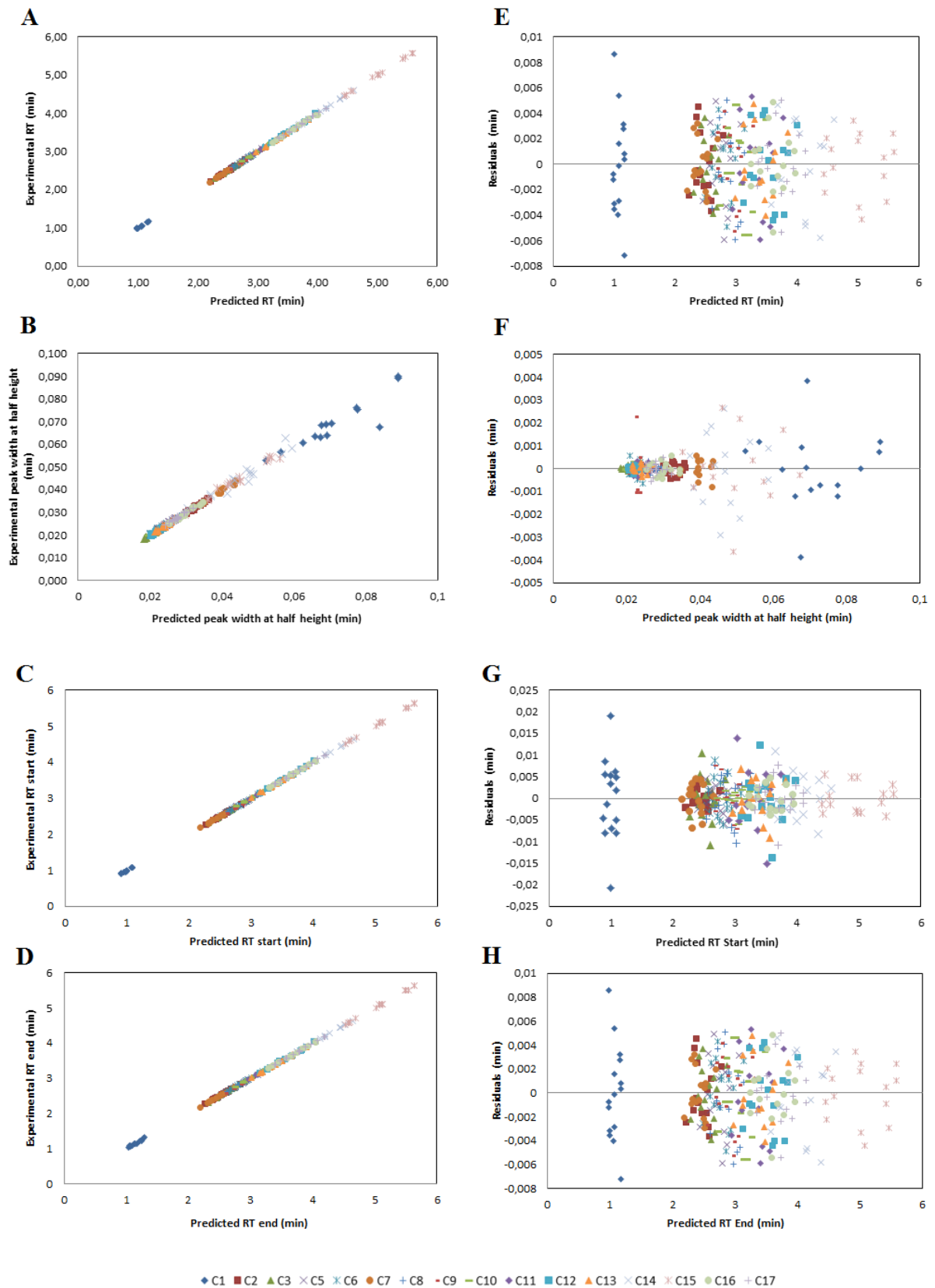


Figure 38: Correlation between experimental responses obtained from DoE and predicted responses: (A) retention time (RT), (B) peak width at half height ($w_{0.5}$), (C) retention time at beginning (RT_{start}) and (D) at the end (RT_{end}) of the peaks. The corresponding residuals distributions for each response and each compound are presented on the left part: (E), (F), (G) and (H) respectively.

In Fig. 37B, experimental and predicted $w_{0,5}$ of C9 (red dash) both fall on a straight line which is an indicator of good model quality. This result was not expected considering the poor R^2_{adj} and p-value. According to their strong correlation, the $w_{0,5}$ model of C9 was therefore not excluded from this study. In the same figure, C14 data (grey crosses) was observed to be slightly out of the straight line for some conditions among the 15 points. However, the good distribution of residuals (Fig. 37F) allowed accepting the model although its quality was not perfect.

The corresponding residuals were normally distributed as shown in Fig. 37E-H. Indeed, no curvature or trend was detected which meant that there were no missing terms in the models. As a reminder, residuals represent the variability between experiments and model predictions and they were all included within a narrow range. Therefore, it is reasonable to assume that the prediction error was really low over the whole experimental domain.

2.2. Design space and optimal chromatographic condition selection

Once the model was validated, the minimal Rs and the minimal S were extracted from all Rs and S calculated for all consecutive peaks of the 216 conditions. They were compared with the number of coeluted peaks predicted to access the design space.

2.2.1. Resolution criterion (Rs)

The design space (DS) was identified in the experimental region (Table 15) where the %H₂O and the BP were both set in a range between -1 and -0.6. Indeed, the minimal number of peak coelution was observed to be higher than 3 for the rest of the explored experimental domain. The graphical representation of the Rs experimental region when the percentage is set at -1 (2% H₂O) with variable BP and t_G is depicted in Fig. 38. The minimal resolution at each condition was observed to be improved as the GT became shorter (Table 15). A compromise had to be made between the minimal Rs and the number of coeluted peaks. The optimal condition was finally selected as follows: the percentage of H₂O as additive set at 2% (-1), the backpressure at 120bar (-1) and the gradient time at 5.4 min (-0.6). The two coelutions for this condition were referred to C1-C7 (Rs=1.09) and C11-C13 (Rs=1.01).

Table 13: Design space identified for CQA Rs. The best condition as a compromise in term of minimal resolution and number of coelutions is shown in the red frame.

y1 (%H2O)	-1	-1	-1	-1	-1	-1	-1	-1	-1	-1	-1	-1
y2 (BP)	-1	-1	-1	-1	-1	-1	-0,6	-0,6	-0,6	-0,6	-0,6	-0,6
y3 (GT)	-1	-0,6	-0,2	0,2	0,6	1	-1	-0,6	-0,2	0,2	0,6	1
Rs min	1,04	1,01	0,89	0,78	0,67	0,56	0,90	0,94	0,91	0,81	0,70	0,59
# Coelutions	3	2	2	2	2	2	4	3	2	2	2	2

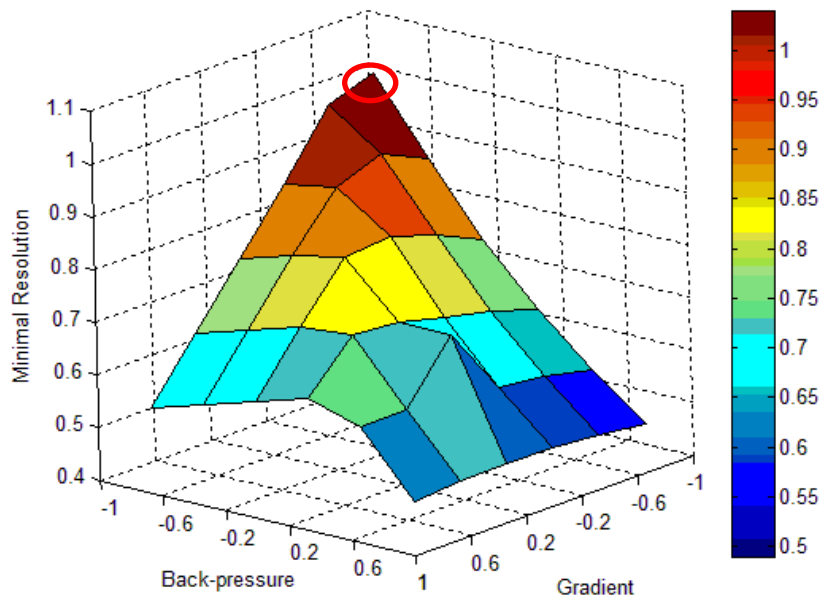


Figure 39: Effect of the two parameters (BP and GT) on the minimal R_s in the experimental region at a constant %H₂O (-1, 2%). Optimal area is presented in the red circle.

2.2.2. Separation criterion (S)

The design space identified when using S as CQA, was similar to the DS, identified when using R_s (Table 16). The same tendency regarding the impact of the three independent parameters on the R_s can be assumed. Indeed, the percentage of water as additive and the backpressure seemed to have a bigger impact in terms of co-elutions as the rest of the experimental domain showed at least 3 coelutions. The separation was observed to be improved as the gradient time became shorter. However, the number of peak coelution is slightly differently predicted while comparing the two criteria. Two conditions were selected as the best compromise between separation and number of peak coelution as shown in Table 16. The graphical representation of the S experimental region when the percentage is set at -1 (2% H₂O) with variable BP and t_G is depicted in Fig. 40. For (-1; -1; -0.6) condition, the two coelutions were referred to C9-C8 ($S = -0.01$) and C11-C13 ($S = -0.02$). The coelution predicted for (-1; -1; 0.6) condition involved C11-C13 ($S = -0.04$).

An observation can be made while comparing the design space by these two approaches. For the same tested conditions, the minimal S varies in a value range of -0.02 to -0.05 whereas the minimal R_s was impacted within a range of 0.4 to 1.1. It suggested that the R_s criterion gives a more precise indication of how much two peaks are coeluted.

Table 14: Design space identified for CQA S. The best conditions as a compromise in term of minimal S and number of coelutions are shown in the red frames.

y1 (%H2O)	-1	-1	-1	-1	-1	-1	-1	-1	-1	-1	-1	-1
y2 (BP)	-1	-1	-1	-1	-1	-0,6	-0,6	-0,6	-0,6	-0,6	-0,6	-0,6
y3 (GT)	-1	-0,6	-0,2	0,2	0,6	1	-1	-0,6	-0,2	0,2	0,6	1
S min	-0,02	-0,02	-0,03	-0,03	-0,04	-0,05	-0,02	-0,02	-0,03	-0,03	-0,04	-0,04
#coelution	4	2	2	2	1	1	4	3	2	2	2	2

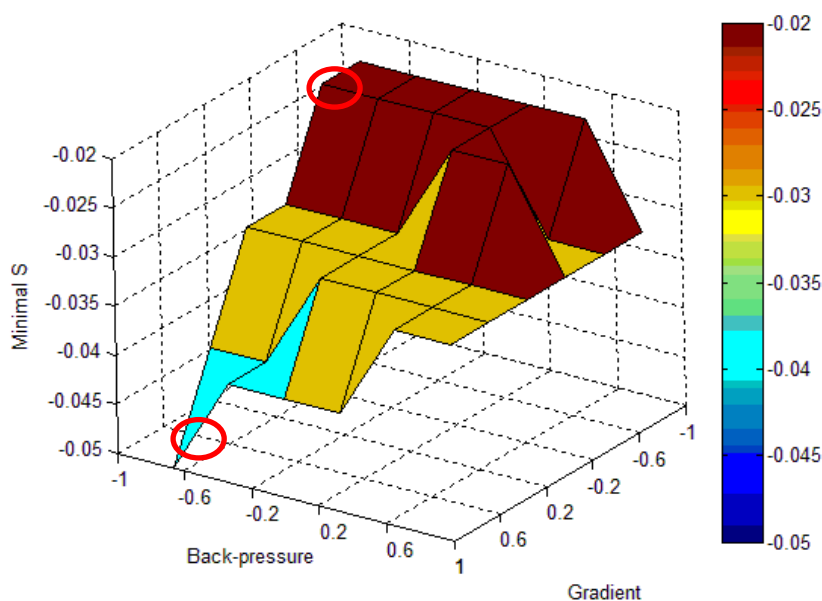


Figure 40 : Effect of the two parameters (BP and GT) on the S factor in the experimental region at a constant %H₂O (-1; 2% H₂O). The predicted optimal areas (-1; -1; -0.6) and (-1; -1; 0.6) are presented in the two red circles.

2.3. Confirmatory experiments

2.3.1. Responses evaluation

The two conditions selected as the best for optimal separation by the two CQAs approaches were experimentally tested. First, there is a strong correlation between predicted and experimental retention time's responses as shown in Fig. 40A; 40C-D. Indeed, the mean relative error percentage (% error) of RT, RT_{start} and RT_{end} were 0.1%; 1.4% and 1.3% respectively. On the other hand, the prediction quality of $w_{0.5}$ was observed to be less good. Indeed the mean % error of $w_{0.5}$ was much higher with a value of 4.2% indicating a clear lack of precision compared to the other responses. This is confirmed in Fig. 40B, where C1, C14 and C15 did not perfectly fit on a straight line. Combined with the variability previously observed in the model quality investigation, the $w_{0.5}$ seemed to be a less good

criterion when dealing with early or late compound elution, which might be impacted by the peak solvent or the increasing modifier. It would be therefore interesting to verify this observation. Further experiments testing other compounds are recommended in the future.

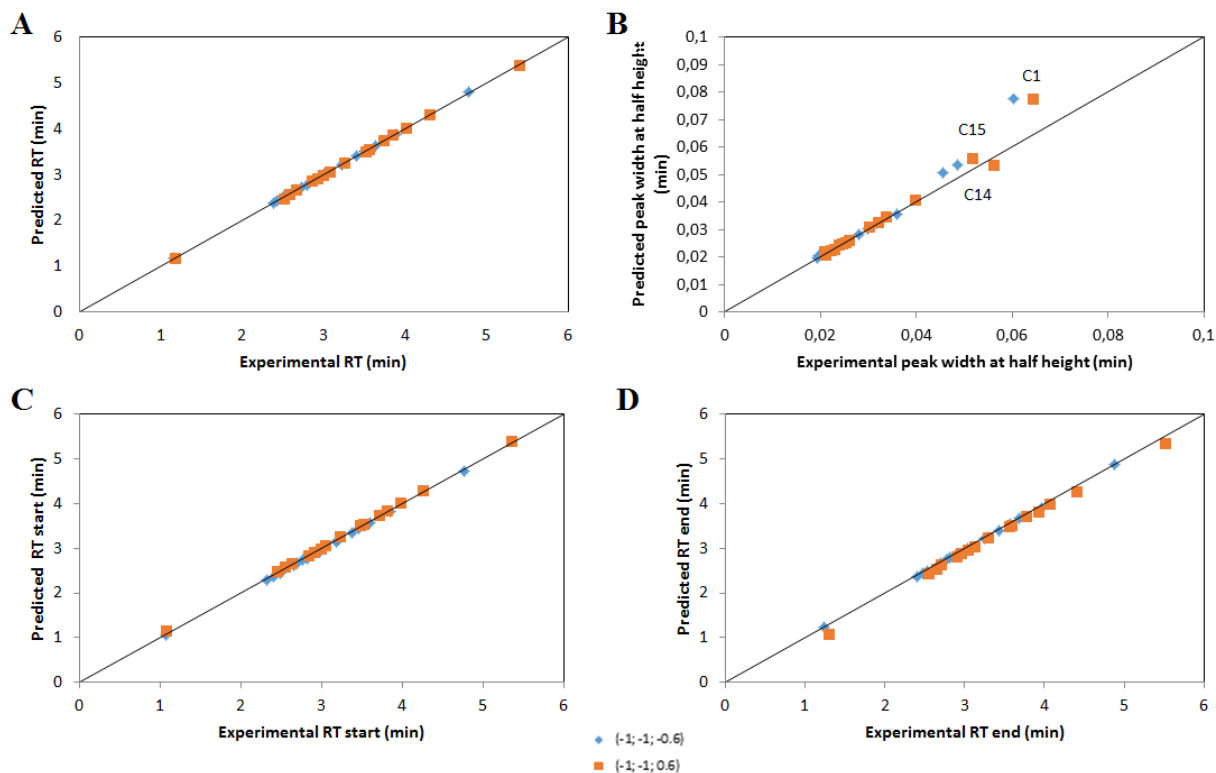


Figure 41: Correlation between experimental responses obtained from DoE and predicted responses at the two optimal conditions: (A) retention time (RT), (B) peak width at half height ($w_{0.5}$), (C) retention time at beginning (RT_{start}) and (D) at the end (RT_{end}) of the peaks. The two conditions (-1; -1; -0.6) and (-1; -1; 0.6) were presented in blue dots and orange square respectively.

2.3.2. R_s and S evaluation

Concerning R_s and S criteria, the comparison of their respective predicted and experimental values are summarized in Table 17. S criterion did not take into account the coelution of C2 and C7 due to the integration processing. Indeed these two compounds coeluted every time and the real RT_{start} and RT_{end} could not be properly extracted from the DoE data results. To tackle this issue, the compounds could be individually injected while performing the DoE. However, this would be very time consuming due to the large number of compounds involved in this study. On the other hand, R_s approach detected the coelution and showed a better separation of these two compounds when the gradient time was longer. This was also observed for C9-C8 which compounds were well separated with the condition (-1; -1; 0.6). The critical pair of peaks C11-C13 was never separated but was less coeluted with a shorter gradient time.

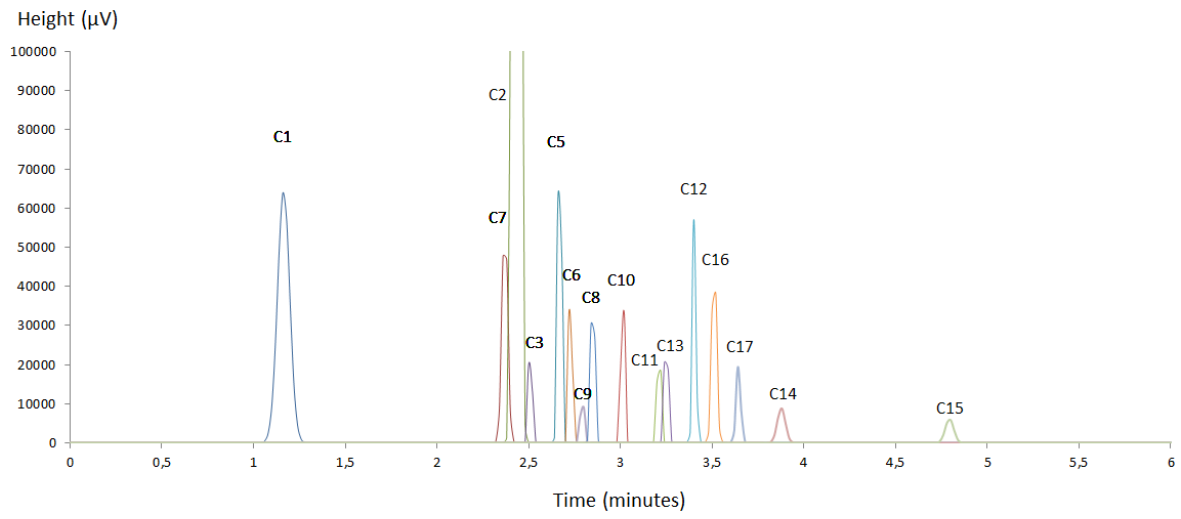
At this point, the comparison of Rs and S criteria is difficult. Indeed, the Rs uncertainties could arise from the $w_{0.5}$ error propagation affecting mainly C1, C14, C15 and the peaks next to it. Moreover, calculation of Rs was made by a division which leads to an even bigger error propagation (by addition of relative errors). On the other hand, S was calculated by a simple subtraction which error corresponds to the absolute errors addition. When S is less liable to be impacted by the responses error, the choice of decimal number could easily change the predictions, potentially questioning the robustness of S criteria. As seen in Table 7, only two decimals were kept leading to an acceptable value of S (equal to 0) when it originally indicated a co-elution (0 values in blue). In fact, it has more influence on S because smaller values are used to indicate a same separation variation than with Rs. In the future, additional investigations are recommended by studying each model terms impact and by removing the least significant terms one by one in order to reduce the model noise. This could be achieved by further statistical analysis. In this way, the refined model could improve the predictions accuracy.

Table 15: Confirmatory experiments for the best condition selected for optimal separation using Rs and S criteria respectively.

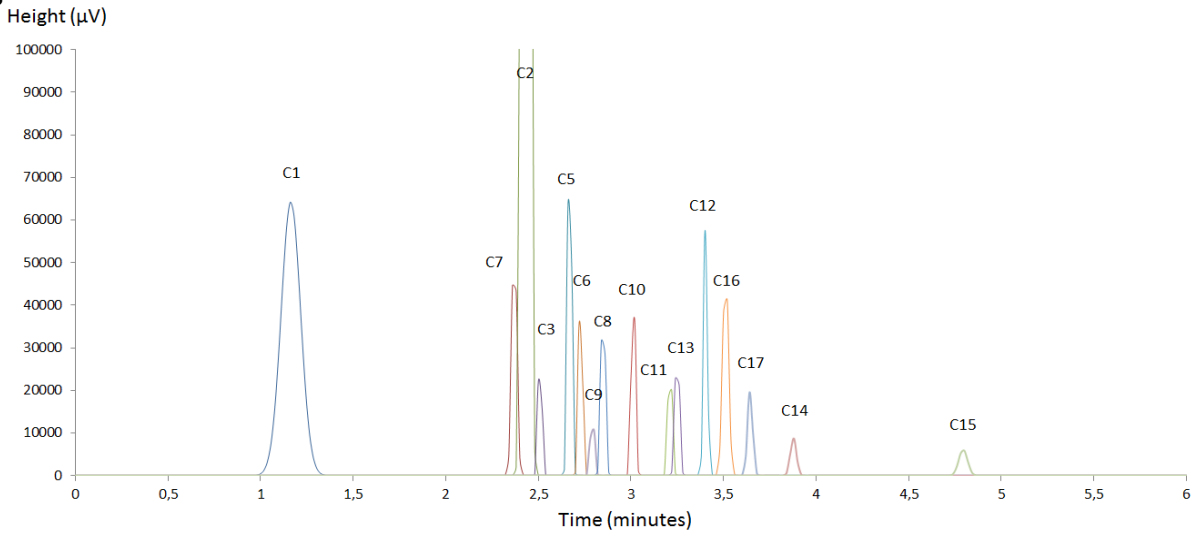
Compounds	(-1; -1; -0.6)				(-1; -1; 0.6)			
	Rs _{pred}	Rs _{exp}	S _{pred}	S _{exp}	Rs _{pred}	Rs _{exp}	S _{pred}	S _{exp}
C1-C7	12,55	14,95	1,15	1,09	13,28	15,18	1,16	1,16
C7-C2	1,09	1,08	0,00	0,00	1,18	1,18	0,00	0
C2-C3	1,74	1,66	0,00	0,00	1,94	1,81	0,01	0,00
C3-C5	4,42	4,43	0,13	0,11	4,85	4,98	0,13	0,134
C5-C6	1,57	1,52	0,00	-0,01	1,59	1,45	0,00	-0,01
C6-C9	1,80	1,87	0,02	0,01	2,05	2,12	0,02	0,021
C9-C8	1,54	1,47	0,00	0,00	1,79	1,92	0,00	0,017
C8-C10	4,28	4,22	0,12	0,10	4,51	4,40	0,12	0,114
C10-C11	5,39	5,51	0,19	0,14	6,36	6,75	0,19	0,199
C11-C13	1,01	0,96	0,04	-0,03	0,67	0,81	-0,04	-0,03
C13-C12	4,08	3,97	0,13	0,09	4,88	4,64	0,13	0,124
C12-C16	2,47	2,29	0,05	0,04	2,46	2,47	0,06	0,048
C1-C17	2,67	2,69	0,06	0,03	2,99	3,07	0,05	0,052
C17-C14	3,49	3,95	0,18	0,16	3,74	4,04	0,17	0,178
C14-C15	10,37	11,50	0,98	0,80	11,84	12,17	0,99	0,945
Rs/S min	1,01	0,96	-0,04	-0,03	0,67	0,81	-0,04	-0,031
#Coelution	2	3	2	2	2	3	1	3

2.4. Optimal separation

A



B



C

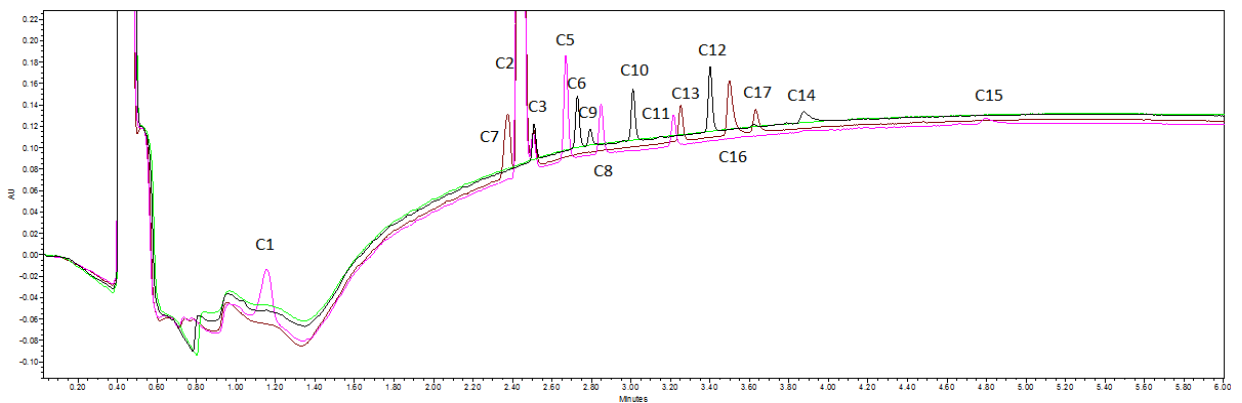


Figure 42: Chromatogram simulated for the predicted optimal parameter (-1; -1; -0.6) by using (A) the height, RT and $w_{0.5}$ for the predicted optimal parameters (-1; -1; -0.6). (B) the height, RT_{start} , RT_{end} and RT. (C) Chromatogram obtained by confirmatory experiments for the same condition: blank (in green), Mix 1 (in black), Mix 2 (in pink) and Mix 3 (in red). The two Time-axes were scaled in the same way

For the predicted optimal parameters (-1; -1; -0.6), the chromatograms obtained by (A) prediction simulation using Rs responses, (B) prediction simulation using S responses and (C) experiments are presented in Fig. 41. Although Rs and S were not perfectly predicted, there were global good correlations between the retention times predicted and experimentally obtained. Fig 41B showed a larger baseline width compared to Fig. 39A. The experiments presented a slight Mix 2 and Mix 3 baseline drift compared to the blank. As a good practice, it is therefore recommended to do one or several replicated experiment(s) on another SFC instrument.

The condition (-1; -1; 0.6) was also investigated by chromatogram simulation (Fig. 42A) and by experiments (Fig. 42B). A better separation of C2-C7 and C8-C9 were confirmed making this condition, the preferred one. Indeed, C2 was a predominant peak and required to be well separated. The resulting optimal chromatographic condition included the use of MeOH and 2% of H₂O as co-solvent, a 6.6 min gradient time and a backpressure kept at 120bars.

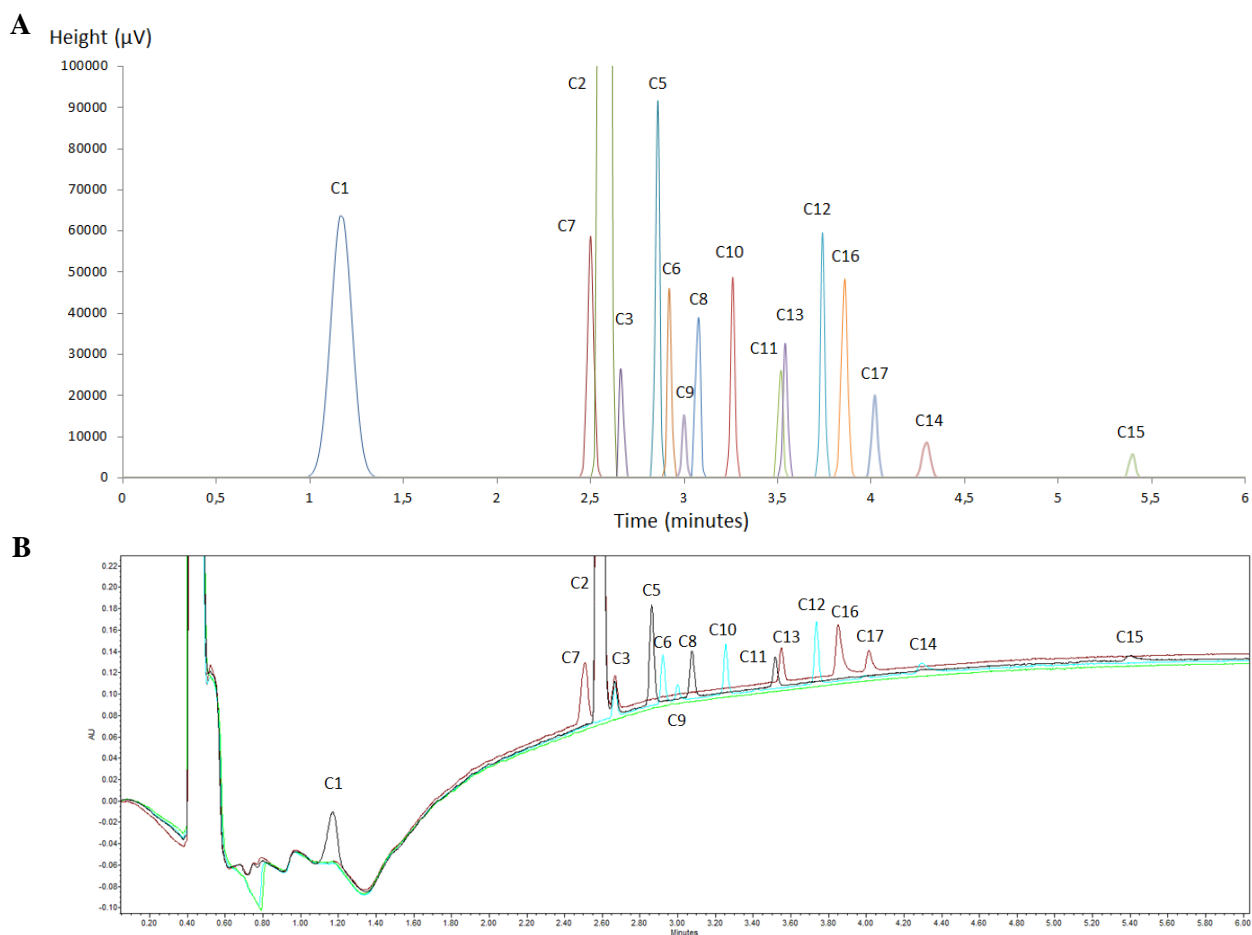


Figure 43: (A) Chromatogram simulated by using the height, RT_{start} , RT_{end} and RT for the predicted optimal parameter (-1; -1; 0.6). (B) Chromatogram obtained by confirmatory experiments for the same condition: blank (in green), Mix 1 (in black), Mix 2 (in pink) and Mix 3 (in red). The two Time-axes were scaled in the same way.

Although some improvements possibilities were tested by adding an isocratic step and a fraction of ACN in organic phase with a trial and error approach, the impurities separation could not be better optimized with the parameters resulting from the screening study. Another possibility would be to test another columns and couple two columns of different chemistries. This option would therefore require a new optimization DoE.

Despite the fact that this method was not able to separate all the peaks, the 17 drug compounds were eluted in less than 7 min gradient time. At UCB Pharma, the possibility of UPLC to separate these 17 compounds was also investigated. The developed method (confidential) was also not able to separate all impurities (Fig. 44). On the other hand, the compound selectivity is different. Hence, SFC can offer an orthogonal method for the separation of some compounds. Also some compounds were observed to be eluted in several peaks (i.e. C13) making the separation by UPLC even more challenging. Furthermore, the long run analysis (25 min of gradient time) is time and solvent consuming compared to the SFC method developed during this study.

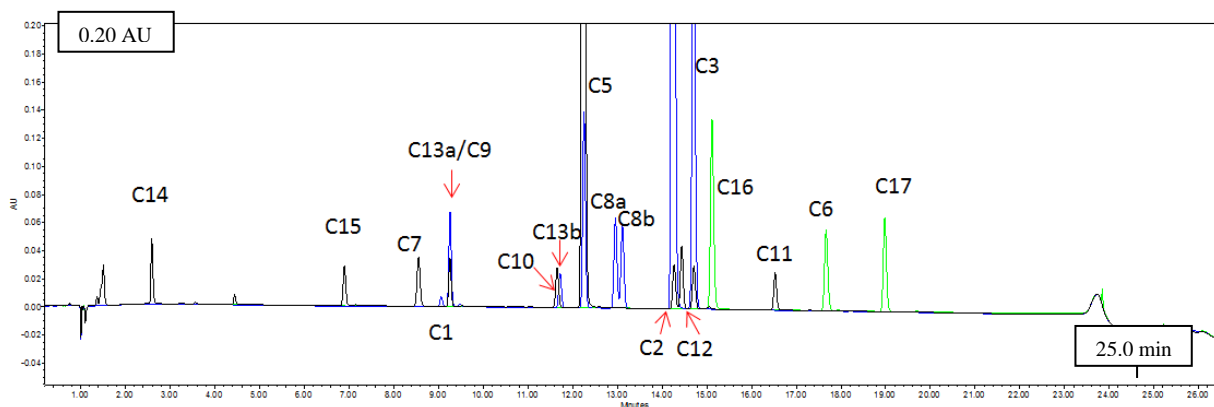


Figure 44: Chromatogram of a method developed by UPLC for the same compounds: mixture of brivaracetam and its impurities.

VI. Conclusion

The present study attested the possibilities of using SFC associated to DoE and computer-assisted optimization methodology for impurities profiling.

The first step included a screening of six different injection solvents, seven stationary phase chemistries and 3 mobile phase compositions. In this context, their advantages were demonstrated in terms of tailing factor, peak capacity and peak height. All aprotic solvents were promising by providing acceptable peak shapes. The use of an organic additive was not required for this study. Different columns chemistries were evaluated and many of them offered good peak shapes. These observations illustrated the flexibility of SFC.

With regards to the objective of method optimization, two approaches were investigated: Rs and S CQAs. Both criteria led to similar design space prediction. However, some discrepancies were highlighted. Firstly, the low relative error values of S-related responses, RT_{start} and RT_{end} (1.4% and 1.3% respectively) boded good model quality. The $w_{0.5}$ model was shown to be less efficient while dealing with early or late compounds elution, suggesting that the effect of peak solvent or increasing modifier consequently impacted the $w_{0.5}$. However, additional experiments are recommended to confirm this observation. Secondly, the S-criteria can be influenced by the developer's choices (i.e. number of decimals) leading to unstable predictions. In the end, there is no best approach; each criterion has its own advantages and drawbacks.

Finally, the optimal method condition was defined when maintaining the backpressure at 120 bar, the gradient time at 6.6 min and when using a mobile phase composed of mainly CO₂ and methanol with 2% of H₂O. Such method is less time and solvent consuming supporting the fast and green interest of SFC. To conclude, the combination of SFC with DoE and computer-assisted methodology was once again demonstrated to be a powerful tool and green alternative for method development in the context of impurity profiling.

Bibliography

Abrahamsson, V. and Sandahl, M. (2013) 'Impact of injection solvents on supercritical fluid chromatography', *Journal of Chromatography A*. Elsevier B.V., 1306, pp. 80–88. doi: 10.1016/j.chroma.2013.07.056.

Alexander, A. J. *et al.* (2013) 'Comparison of supercritical fluid chromatography and reverse phase liquid chromatography for the impurity profiling of the antiretroviral drugs lamivudine/BMS-986001/efavirenz in a combination tablet', *Journal of Pharmaceutical and Biomedical Analysis*. Elsevier B.V., 78–79, pp. 243–251. doi: 10.1016/j.jpba.2013.02.019.

Andri, B. *et al.* (2017) 'Optimization and validation of a fast supercritical fluid chromatography method for the quantitative determination of vitamin D3 and its related impurities', *Journal of Chromatography A*. Elsevier B.V., 1491, pp. 171–181. doi: 10.1016/j.chroma.2017.01.090.

Ashraf-Khorassani, M. *et al.* (2015) 'Ultrahigh performance supercritical fluid chromatography of lipophilic compounds with application to synthetic and commercial biodiesel', *Journal of Chromatography B: Analytical Technologies in the Biomedical and Life Sciences*. Elsevier B.V., 983–984, pp. 94–100. doi: 10.1016/j.jchromb.2014.12.012.

Berger, T. A. (1987) 'Supercritical Fluid Chromatography', pp. 1–9.

Berger, T. A. (2015) *Supercritical fluid chromatography*. Agilent Te.

Berger, T. A. and Berger, B. K. (2011) 'Minimizing UV noise in supercritical fluid chromatography. I. Improving back pressure regulator pressure noise', *Journal of Chromatography A*. Elsevier B.V., 1218(16), pp. 2320–2326. doi: 10.1016/j.chroma.2011.02.030.

Bhal, S. K. (2007) 'Application Note: Lipophilicity Descriptors: Understanding When to Use LogP and LogD', *ACD/Labs PhysChem Software Application Notes*. Available online at: http://www.acdlabs.com/resources/knowledgebase/app_notes/physchem/ (accessed 09/09/15), pp. 1–4.

Brunelli, C. *et al.* (2008) 'Development of a supercritical fluid chromatography high-resolution separation method suitable for pharmaceuticals using cyanopropyl silica', *Journal of Chromatography A*, 1185(2), pp. 263–272. doi: 10.1016/j.chroma.2008.01.050.

Byrne, N. *et al.* (2008) 'Analysis and purification of alcohol-sensitive chiral compounds using 2,2,2-trifluoroethanol as a modifier in supercritical fluid chromatography', *Journal of Chromatography B: Analytical Technologies in the Biomedical and Life Sciences*, 875(1), pp. 237–242. doi: 10.1016/j.jchromb.2008.06.057.

Cazenave-Gassiot, A. *et al.* (2008) 'Prediction of retention for sulfonamides in supercritical fluid

chromatography', *Journal of Chromatography A*, 1189(1–2), pp. 254–265. doi: 10.1016/j.chroma.2007.10.020.

Crawford Scientific (no date) *Instrumentation of HPLC detectors*, CHROMAcademy.

Davim, J. P. (2016) *Design of Experiments in Production Engineering, Management and Industrial Engineering*, Springer.

Debrus, B. *et al.* (2011) 'Innovative high-performance liquid chromatography method development for the screening of 19 antimalarial drugs based on a generic approach, using design of experiments, independent component analysis and design space', *Journal of Chromatography A*. Elsevier B.V., 1218(31), pp. 5205–5215. doi: 10.1016/j.chroma.2011.05.102.

Desfontaine, V. *et al.* (2017) 'A systematic investigation of sample diluents in modern supercritical fluid chromatography', *Journal of Chromatography A*. Elsevier B.V., 1511, pp. 1–10. doi: 10.1016/j.chroma.2017.06.075.

Desfontaine, V., Veuthey, J. L. and Guillarme, D. (2016) 'Evaluation of innovative stationary phase ligand chemistries and analytical conditions for the analysis of basic drugs by supercritical fluid chromatography', *Journal of Chromatography A*. Elsevier B.V., 1438, pp. 244–253. doi: 10.1016/j.chroma.2016.02.029.

Dispas, A. *et al.* (2016) 'Screening study of SFC critical method parameters for the determination of pharmaceutical compounds', *Journal of Pharmaceutical and Biomedical Analysis*. Elsevier B.V., 125, pp. 339–354. doi: 10.1016/j.jpba.2016.04.005.

Duval, J. *et al.* (2016) 'Contribution of Supercritical Fluid Chromatography coupled to High Resolution Mass Spectrometry and UV detections for the analysis of a complex vegetable oil – Application for characterization of a *Kniphofia uvaria* extract', *Comptes Rendus Chimie*, 19(9), pp. 1113–1123. doi: 10.1016/j.crci.2015.11.022.

Fairchild, J. N., Hill, J. F. and Iraneta, P. C. (2013) 'Significant peak distortion caused by sample diluent solvents occurs', *LCGC North America*, 31(4), pp. 326–333.

Galea, C., Mangelings, D. and Heyden, Y. Vander (2015) 'Method development for impurity profiling in SFC: THE selection of a dissimilar set of stationary phases', *Journal of Pharmaceutical and Biomedical Analysis*. Elsevier B.V., 111, pp. 333–343. doi: 10.1016/j.jpba.2014.12.043.

GE Healthcare (2014) '29-1038-50 - Design of Experiments in Protein Production and Purification', *General Electric Company*, p. 128. Available at: www.gelifesciences.com/handbooks.

Grand-Guillaume Perrenoud, A., Veuthey, J. L. and Guillarme, D. (2012) 'Comparison of ultra-high performance supercritical fluid chromatography and ultra-high performance liquid chromatography for the analysis of pharmaceutical compounds', *Journal of Chromatography A*. Elsevier B.V., 1266, pp. 158–167. doi: 10.1016/j.chroma.2012.10.005.

Hibbert, D. B. (2012) 'Experimental design in chromatography: A tutorial review', *Journal of Chromatography B: Analytical Technologies in the Biomedical and Life Sciences*. Elsevier B.V., 910, pp. 2–13. doi: 10.1016/j.jchromb.2012.01.020.

Ho, C. S. *et al.* (2003) 'Electrospray ionisation mass spectrometry: principles and clinical applications.', *The Clinical biochemist*, 24(1), pp. 3–12. doi: 10.1146/annurev.bi.64.070195.001531.

Ishibashi, M. *et al.* (2015) 'High-throughput simultaneous analysis of pesticides by supercritical fluid chromatography coupled with high-resolution mass spectrometry', *Journal of Agricultural and Food Chemistry*, 63(18), pp. 4457–4463. doi: 10.1021/jf5056248.

De Klerck, K., Vander Heyden, Y. and Manglings, D. (2013) 'Advances in supercritical fluid chromatography for the analysis of chiral and achiral pharmaceuticals', *LC GC Europe*, 26(5 SUPPL.), p. 6. Available at: www.chromatographyonline.com.

Lemasson, E. *et al.* (2015) 'Development of an achiral supercritical fluid chromatography method with ultraviolet absorbance and mass spectrometric detection for impurity profiling of drug candidates. Part I: Optimization of mobile phase composition', *Journal of Chromatography A*. Elsevier B.V., 1408, pp. 217–226. doi: 10.1016/j.chroma.2015.07.037.

Lesellier, E. and West, C. (2015) 'The many faces of packed column supercritical fluid chromatography - A critical review', *Journal of Chromatography A*. Elsevier B.V., 1382, pp. 2–46. doi: 10.1016/j.chroma.2014.12.083.

Menet, M.-C. (2011) *RFL - revue francophone des laboratoires.*, /data/revues/1773035X/00410437/41/. Elsevier Masson. Available at: <http://www.em-consulte.com/en/article/678574> (Accessed: 16 August 2017).

Müllertz, A., Perrie, Y. and Rades, T. (2016) *Analytical techniques in the pharmaceutical sciences*. doi: 10.1017/CBO9781107415324.004.

Muscat Galea, C., Mangelings, D. and Vander Heyden, Y. (2017) 'Investigation of the effect of mobile phase composition on selectivity using a solvent-triangle based approach in achiral SFC', *Journal of Pharmaceutical and Biomedical Analysis*. Elsevier B.V., 132, pp. 247–257. doi: 10.1016/j.jpba.2016.10.016.

Neue, U. D. (2005) 'Theory of peak capacity in gradient elution', *Journal of Chromatography A*, 1079(1–2 SPEC. ISS.), pp. 153–161. doi: 10.1016/j.chroma.2005.03.008.

Nie, L., Dai, Z. and Ma, S. (2016) 'Improved Chiral Separation of (R,S)-Goitrin by SFC: An Application in Traditional Chinese Medicine', *Journal of Analytical Methods in Chemistry*, 2016. doi: 10.1155/2016/5782942.

Nováková, L. *et al.* (2014) 'Modern analytical supercritical fluid chromatography using columns packed with sub-2 μ m particles: A tutorial', *Analytica Chimica Acta*. Elsevier B.V., 824, pp. 18–35. doi: 10.1016/j.aca.2014.03.034.

Rafamantanana, M. H. *et al.* (2012) 'Application of design of experiments and design space methodology for the HPLC-UV separation optimization of aporphine alkaloids from leaves of *Spirospermum penduliflorum* Thouars', *Journal of Pharmaceutical and Biomedical Analysis*, 62, pp. 23–32. doi: 10.1016/j.jpba.2011.12.028.

Ratsameepakai, W. *et al.* (2015) 'Evaluation of ultrahigh-performance supercritical fluid chromatography-mass spectrometry as an alternative approach for the analysis of fatty acid methyl esters in aviation turbine fuel', *Energy and Fuels*, 29(4), pp. 2485–2492. doi:

10.1021/acs.energyfuels.5b00103.

Robert M. Silverstein, Francis X. Webster, D. J. K. (2005) *Spectrometric identification of organic compounds*, *Journal of Molecular Structure*. doi: 10.1016/0022-2860(76)87024-X.

Tiwari, G. and Tiwari, R. (2010) 'Bioanalytical method validation: An updated review.', *Pharmaceutical methods*. Wolters Kluwer -- Medknow Publications, 1(1), pp. 25–38. doi: 10.4103/2229-4708.72226.

U.S. Department of Health and Human Services Food and Drug Administration (2009) 'ICH Q8(R2) Pharmaceutical Development', *Workshop: Quality by Design in pharmaceutical*, 8(November), p. 28.

US Pharmacopeia (no date) '{ 621 } Chromatography', 1(2).

Wang, C., Tymiak, A. A. and Zhang, Y. (2014) 'Optimization and simulation of tandem column supercritical fluid chromatography separations using column back pressure as a unique parameter', *Analytical Chemistry*, 86(8), pp. 4033–4040. doi: 10.1021/ac500530n.

'Waters SFC preparative' (no date).

West, C. (2013) 'How Good is SFC for Polar Analytes?', *Chromatography Today*, pp. 22–27.

West, C. *et al.* (2015) 'Sum of ranking differences to rank stationary phases used in packed column supercritical fluid chromatography', *Journal of Chromatography A*. Elsevier B.V., 1409, pp. 241–250. doi: 10.1016/j.chroma.2015.07.071.

West, C. *et al.* (2016) 'An improved classification of stationary phases for ultra-high performance supercritical fluid chromatography', *Journal of Chromatography A*. Elsevier B.V., 1440, pp. 212–228. doi: 10.1016/j.chroma.2016.02.052.

West, C. and Lesellier, E. (2013) 'Effects of mobile phase composition on retention and selectivity in achiral supercritical fluid chromatography', *Journal of Chromatography A*. Elsevier B.V., 1302, pp. 152–162. doi: 10.1016/j.chroma.2013.06.003.

'WHO | Epilepsy' (2017) *WHO*. World Health Organization. Available at: <http://www.who.int/mediacentre/factsheets/fs999/en/> (Accessed: 16 August 2017).

Zheng, J., Taylor, L. T. and Pinkston, J. D. (2006) 'Elution of cationic species with/without ion pair reagents from polar stationary phases via SFC', *Chromatographia*, 63(5–6), pp. 267–276. doi: 10.1365/s10337-006-0731-z.